

Timing of centrosome separation is important for accurate chromosome segregation

William T. Silkworth^a, Isaac K. Nardi^{a,*}, Raja Paul^b, Alex Mogilner^c, and Daniela Cimini^a

^aDepartment of Biological Sciences, Virginia Tech, Blacksburg, VA 24061; ^bIndian Association for the Cultivation of Science, Jadavpur, Kolkata 700032, India; ^cDepartment of Neurobiology, Physiology and Behavior and Department of Mathematics, University of California, Davis, Davis, CA 95616

ABSTRACT Spindle assembly, establishment of kinetochore attachment, and sister chromatid separation must occur during mitosis in a highly coordinated fashion to ensure accurate chromosome segregation. In most vertebrate cells, the nuclear envelope must break down to allow interaction between microtubules of the mitotic spindle and the kinetochores. It was previously shown that nuclear envelope breakdown (NEB) is not coordinated with centrosome separation and that centrosome separation can be either complete at the time of NEB or can be completed after NEB. In this study, we investigated whether the timing of centrosome separation affects subsequent mitotic events such as establishment of kinetochore attachment or chromosome segregation. We used a combination of experimental and computational approaches to investigate kinetochore attachment and chromosome segregation in cells with complete versus incomplete spindle pole separation at NEB. We found that cells with incomplete spindle pole separation exhibit higher rates of kinetochore misattachments and chromosome missegregation than cells that complete centrosome separation before NEB. Moreover, our mathematical model showed that two spindle poles in close proximity do not “search” the entire cellular space, leading to formation of large numbers of syntelic attachments, which can be an intermediate stage in the formation of merotelic kinetochores.

Monitoring Editor
Yixian Zheng
Carnegie Institution

Received: Feb 2, 2011
Revised: Nov 17, 2011
Accepted: Nov 22, 2011

INTRODUCTION

Accurate chromosome segregation during mitosis is critical to maintain genome stability and prevent aneuploidy. To this aim, assembly of the mitotic spindle must be coordinated with establishment of kinetochore (KT) attachment. The microtubules (MTs) of a bipolar mitotic spindle must interact with the chromosomes so that the two sister KTs on each chromosome interact with opposite spindle poles. This configuration will allow the two sister chromatids to be pulled to opposite ends of the cell upon sister chromatid separation, thus leading to the formation of two daughter cells with the correct chromosome number.

This article was published online ahead of print in MBoC in Press (<http://www.molbiolcell.org/cgi/doi/10.1091/mbc.E11-02-0095>) on November 30, 2011.

*Present address: Department of Molecular Cell and Developmental Biology, University of Virginia School of Medicine, Charlottesville, VA 22908.

Address correspondence to: Daniela Cimini (cimini@vt.edu).

Abbreviations used: KT, kinetochore; MT, microtubule; NEB, nuclear envelope breakdown; NOC, nocodazole; STLC, S-trityl-L-cysteine.

© 2012 Silkworth et al. This article is distributed by The American Society for Cell Biology under license from the author(s). Two months after publication it is available to the public under an Attribution–Noncommercial–Share Alike 3.0 Unported Creative Commons License (<http://creativecommons.org/licenses/by-nc-sa/3.0>).

“ASCB®,” “The American Society for Cell Biology®,” and “Molecular Biology of the Cell®” are registered trademarks of The American Society of Cell Biology.

In most higher eukaryote cells interaction between spindle MTs and chromosomes is possible only after nuclear envelope breakdown (NEB). In fact, the nuclear envelope disassembles in early mitosis, and it is only after NEB that the MTs emanating from the centrosomes (spindle poles) can interact with the KTs. It has been known for many years that centrosome separation is not coordinated with NEB (Mole Bajer, 1975; Rattner and Berns, 1976). Indeed, in several different cell types centrosome separation is completed before NEB in ~50% of mitotic cells within the same cell population, whereas in the other 50% centrosome separation is completed after NEB (Rattner and Berns, 1976; Aubin et al., 1980; Waters et al., 1993; Whitehead et al., 1996; Rosenblatt et al., 2004; Toso et al., 2009). Several studies showed that both the pre-NEB centrosome separation, referred to as the prophase pathway, and the post-NEB centrosome separation, referred to as the prometaphase pathway, rely on Eg5-dependent MT sliding (Whitehead and Rattner, 1998; Sharp et al., 1999; Rosenblatt, 2005; Tanenbaum et al., 2008; Tanenbaum and Medema, 2010; Woodcock et al., 2010). However, other mechanisms are specific to each of the two pathways (reviewed in Rosenblatt, 2005; Tanenbaum and Medema, 2010). A major mechanism of prophase centrosome separation involves the interaction between astral MTs and the nuclear

envelope, possibly mediated by dynein (Gonczy *et al.*, 1999; Robinson *et al.*, 1999; Rosenblatt, 2005; Tanenbaum and Medema, 2010), whereas centrosome separation during prometaphase requires myosin activity at the cell cortex (Rosenblatt *et al.*, 2004; Rosenblatt, 2005; Tanenbaum and Medema, 2010).

Whereas many studies have focused on identifying the molecules and mechanisms required for centrosome separation during these two mitotic stages, it is not known whether incomplete spindle pole separation at NEB will affect subsequent mitotic events such as establishment of KT attachment or chromosome segregation. When centrosomes achieve complete separation in prophase, at NEB the two spindle poles will be at opposite ends of the nuclear space and the MTs will grow from the centrosomes toward the chromosomes symmetrically. Conversely, when the centrosomes are not completely separated at NEB, the two spindle poles will be shifted to one side of the nuclear space and MT growth toward the chromosomes will be asymmetrical. On the basis of these differences, we speculated that incomplete spindle pole separation at NEB might lead to erroneous KT attachment and possibly chromosome missegregation. To test this hypothesis, we used a combination of experimental and computational approaches and investigated KT attachment and chromosome segregation in PtK1 cells with complete versus incomplete spindle pole separation at NEB. We found that cells with incomplete spindle pole separation at NEB exhibit KT misattachments and chromosome missegregation. In addition, our mathematical model showed that two spindle poles in close proximity do not “search” the entire cellular space, and this leads to formation of large numbers of syntelic attachments, which can be an intermediate stage in the formation of merotelic KTs.

RESULTS

Incomplete spindle pole separation at NEB is associated with elevated frequencies of anaphase lagging chromosomes

We first wanted to test the hypothesis that incomplete spindle pole separation at NEB causes KT misattachments and chromosome missegregation. Of all possible KT misattachments (monotelic, syntelic, and merotelic), merotelic attachments (a single KT bound to MTs from two spindle poles instead of just one) are known for not

being detected by the spindle assembly checkpoint (Khodjakov *et al.*, 1997a; Wise and Brinkley, 1997; Yu and Dawe, 2000; Cimini *et al.*, 2002, 2004) and can therefore persist through mitosis into anaphase, when they can induce anaphase lagging chromosomes (Cimini *et al.*, 2001, 2004). Thus an easy way to test our hypothesis was to determine whether increased frequencies of anaphase lagging chromosomes are found in cells with incomplete versus complete spindle pole separation at NEB. To this aim, we used PtK1 cells expressing green fluorescent protein (GFP)- γ -tubulin (a generous gift from Alexey Khodjakov, Wadsworth Center, Albany, NY; Khodjakov *et al.*, 1997b). Although these cells were previously shown (Cimini *et al.*, 2003b; W. T. Silkworth and D. Cimini, unpublished results) to complete centrosome separation before NEB >90% of the time, we fortuitously isolated a subclone of this cell line that exhibited incomplete spindle pole separation at NEB at higher rates and used it for this study. We performed time-lapse experiments in which the cells were imaged from prophase through late anaphase. To discriminate between complete and incomplete spindle pole separation at NEB, we measured the pole-to-pole distance upon NEB (see *Materials and Methods* for details) and at the end of prometaphase. Moreover, we determined the positioning of the centrosomes with respect to the chromosomes prior to and upon NEB. We found that the configuration of centrosome positioning with respect to the chromosomes prior to NEB could fall into four different categories, as diagrammed in Figure 1A, i–iv. In two of these categories (Figure 1A, i and ii), cells exhibited complete centrosome separation prior to NEB, but in one case the centrosomes were positioned along an axis parallel to the substrate (Figures 1A, i, and 2A), whereas in the other the centrosomes were positioned along an axis perpendicular to the substrate (Figure 1A, ii, Supplemental Figure S1A, and Figure 2B). Of note, in the latter category the centrosomes repositioned to the central region of the nuclear space at the time of NEB (Figure 1B, ii, Supplemental Figure S1A, and Figure 2B), thus reverting to an unseparated state. In the other two groups either the centrosomes were positioned at the edge of the nuclear space (Figure 1, A and B, iii, Supplemental Figure S1B, and Figure 2C) or one centrosome was positioned at the edge of the nuclear space and the other on the top surface of the nuclear space (Figure 1A, iv, Supplemental Figure S1C, and

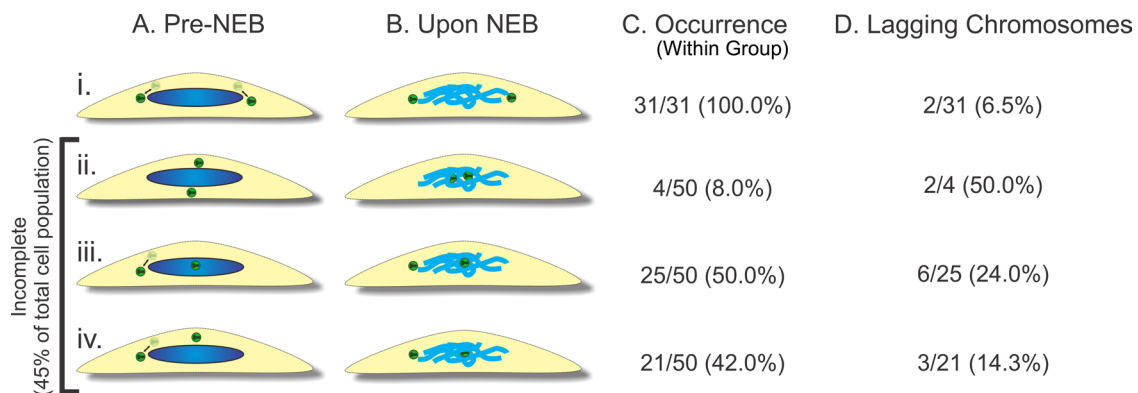


FIGURE 1: Analysis of centrosome positioning before and immediately after NEB. (A, B) Diagrams showing the different types of centrosome arrangements before (A) and upon NEB (B) in PtK1 cells with complete (i) or incomplete (ii–iv) centrosome separation. The arrow between a shadowed and a dark image of the centrosome in i, iii, and iv indicates that the centrosome could be positioned at any point between the two. Note that in those cases in which the centrosomes achieve positions at the top and bottom of the nucleus before NEB (A, ii), they do not persist in such positions upon NEB, and instead they move toward the center of the nuclear space. See Supplemental Figure S1 for examples of cells with different centrosome configurations. (C) Rates of occurrence of the various configurations of centrosome positioning within the complete (i) and incomplete (ii–iv) spindle pole separation groups. (D) Rates of anaphase lagging chromosomes in cells from each subgroup.

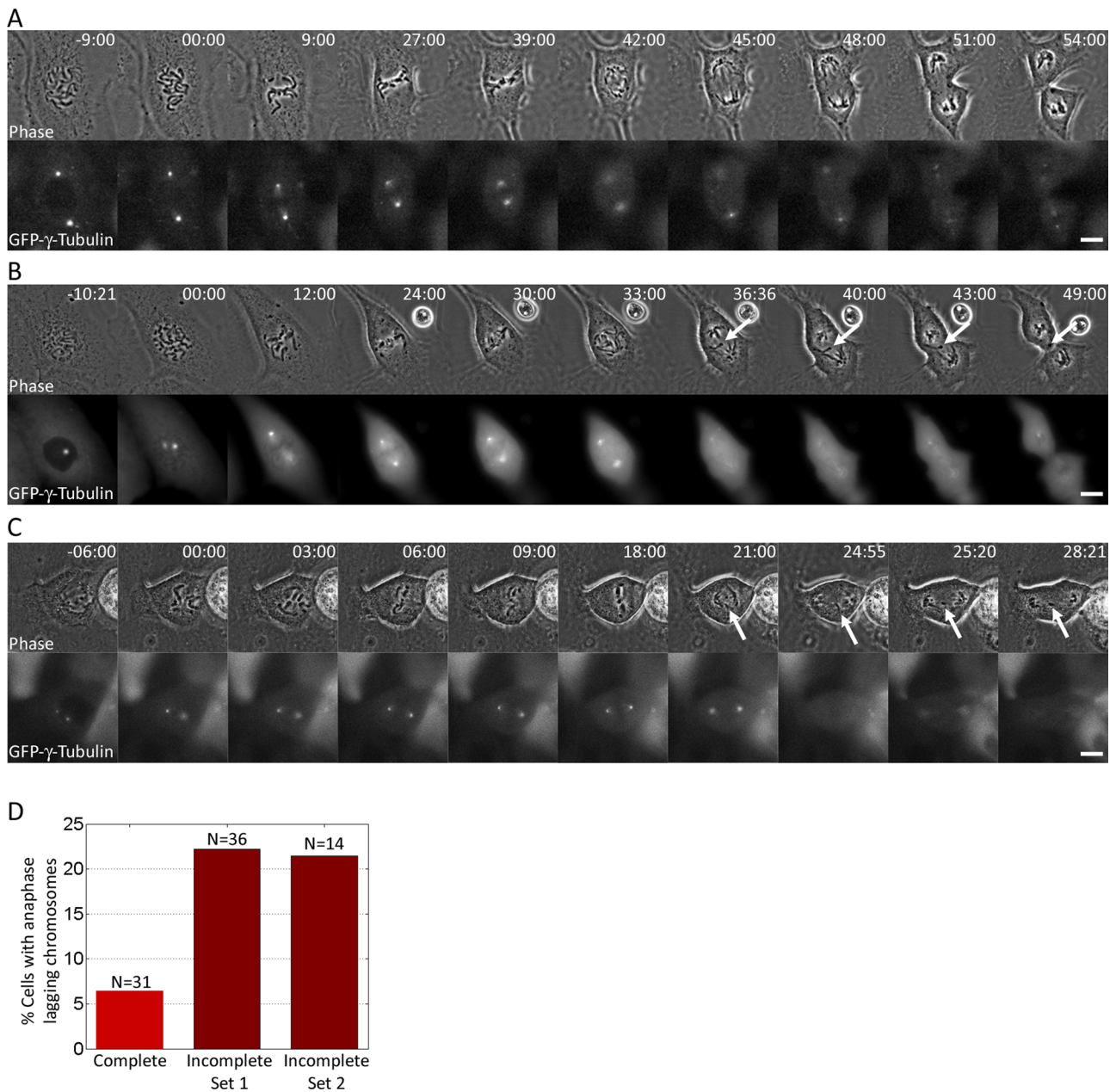


FIGURE 2: Incomplete spindle pole separation at NEB is associated with elevated frequencies of anaphase lagging chromosomes. (A–C) Still images from time-lapse movies of PtK1 cells expressing GFP- γ -tubulin. Phase-contrast images are shown in the top row and single focal plane GFP images are shown in the bottom row. A cell in which the spindle poles were fully separated at NEB is shown in A. In the cell shown in B, the centrosomes were separated along the z-axis of the cell prior to NEB (–10:21-min time point; only one centrosome is in focus in the image) but moved toward the center of the nuclear space and in very close proximity upon NEB (00:00-min time point). The same cell exhibits an anaphase lagging chromosome (arrow). In the cell shown in C, the centrosomes were shifted to one side of the nuclear space prior to and upon NEB. One lagging chromosome (arrow) was present in anaphase. (D) Frequencies of anaphase lagging chromosomes in cells with complete and incomplete spindle pole separation at NEB. The Incomplete Set 2 data refer to an additional set of cells with incomplete centrosome separation imaged by four-dimensional (three-dimensional plus time) time-lapse microscopy (see *Materials and Methods* for details). Scale bars, 10 μ m.

Figure 3B). In the latter case, the centrosome on the top surface repositioned toward the center of the nuclear space upon NEB (Figure 1B, iv, and Supplemental Figure S1C). Because of the reduced pole-to-pole distance upon NEB (i.e., the time when kinetochore–microtubule interaction becomes possible), cells displaying centrosome configurations like those depicted in Figure 1B, ii–iv (and shown in Supplemental Figure S1), were classified as cells with

incomplete centrosome separation. Cells with complete centrosome separation displayed centrosome positioning like that depicted in Figure 1B, i (and shown in Figures 2A and 3A). After an initial characterization of centrosome positioning in the overall population, an additional set of cells with incomplete centrosome separation was selectively imaged (see *Materials and Methods* for details) to confirm the results obtained in the initial screening.

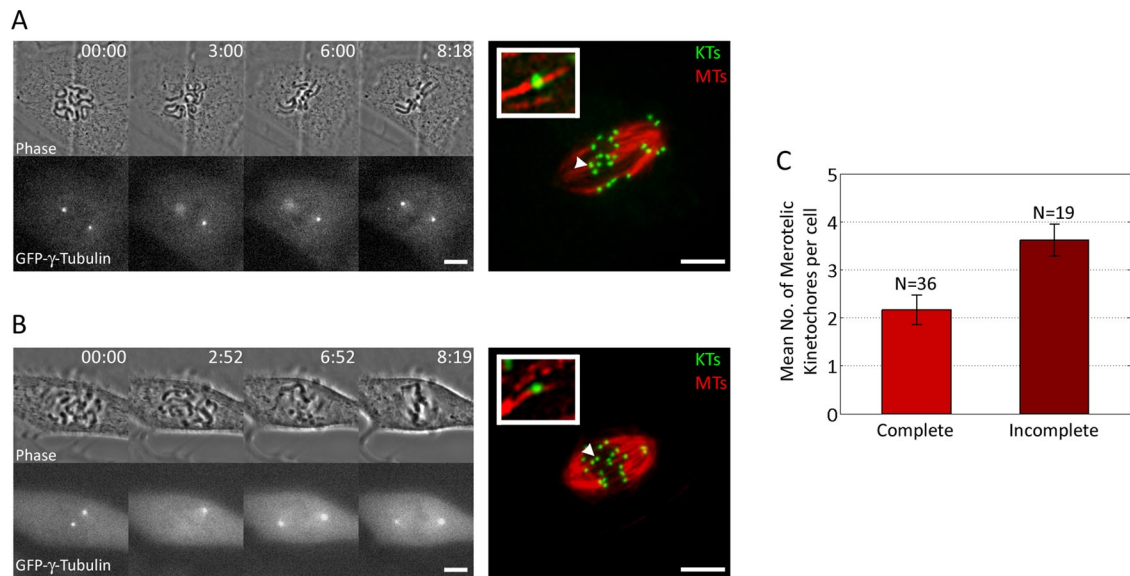


FIGURE 3: Incomplete spindle pole separation at NEB promotes formation of merotelic kinetochore attachments. (A, B) Examples of GFP- γ -tubulin PtK1 cells imaged by time-lapse microscopy from NEB to late prometaphase, then immunostained for KT and MTs, relocalized, and imaged by confocal microscopy (far right). A cell with complete spindle pole separation at NEB is shown in A, whereas a cell with incomplete spindle pole separation is shown in B. Insets represent 225% enlargements of the KTs indicated by the arrowheads. (C) The histogram shows that prometaphase cells with incomplete spindle pole separation at NEB exhibit higher (*t* test, $p < 0.01$) numbers of merotelic KTs than do cells with complete spindle pole separation at NEB. Error bars represent standard errors of the mean. Scale bars in the time-lapse images, 10 μ m. Scale bars in the fixed cell images, 5 μ m.

When all the data were taken together, we found that for cells with incomplete centrosome separation the mean interpolar distance upon NEB was 7.33 ± 2.02 (mean \pm SD; $N = 50$), which was $<75\%$ the distance measured at the end of prometaphase (13.63 ± 1.98 μ m; Supplemental Figure S2). In cells with complete centrosome separation the mean pole-to-pole distance was 15.81 ± 4.99 μ m ($N = 31$) upon NEB and 12.63 ± 1.97 μ m at the end of prometaphase. Our measurements are consistent with previously reported pole-to-pole distances of 12–15 μ m in metaphase PtK1 cells (Brinkley and Cartwright, 1971; Cameron *et al.*, 2006). We also measured the distance across the long axis of the “nuclear space” (i.e., region occupied by the chromosomes) at NEB and found an average size of 16.27 ± 3.39 μ m ($N = 67$). This indicates that, whereas in cells with complete spindle pole separation the centrosomes were positioned at opposite ends of the nuclear space, in cells with incomplete spindle pole separation, the pole-to-pole distance at NEB was less than half that of the nuclear space. This suggests that the positioning of the centrosomes in such cells may cause a single KT to face both spindle poles and thus establish a merotelic attachment, which, if not corrected, will result in a lagging chromosome in anaphase. Indeed, cells with incomplete spindle pole separation upon NEB exhibited high frequencies of anaphase lagging chromosomes, which overall were ~ 3.5 -fold the frequency of anaphase lagging chromosomes in cells with complete spindle pole separation (Figures 1D and 2D). In agreement with previous observations (Toso *et al.*, 2009), there was no significant difference in the duration of mitosis for cells with complete versus incomplete spindle pole separation (data not shown). Consistently, numerical simulations showed that at small initial distances between spindle poles, there are more persistent merotelic attachments, but those do not induce a mitotic delay (Cimini *et al.*, 2002). Monotelic attachments, which can cause a mitotic delay, dis-

appear in the simulations just 2–3 min more slowly in cells with incomplete spindle pole separation compared with cells with initial pole-to-pole distances of 12–15 μ m, thus delaying mitosis insignificantly. Taken together, these data reveal that cells that start prometaphase with incompletely separated centrosomes/spindle poles are more likely than those with complete spindle pole separation to exhibit chromosome segregation defects in the form of anaphase lagging chromosomes (Figures 1D and 2).

Incomplete spindle pole separation at NEB promotes formation of merotelic kinetochore attachments

Differences in frequencies of anaphase lagging chromosomes may be due to either differences in the rate of formation (Cimini *et al.*, 2001, Cimini *et al.*, 2003b; Kline-Smith *et al.*, 2004; Salmon *et al.*, 2005; Ganem *et al.*, 2009; Silkworth *et al.*, 2009) or differences in the rate of correction of merotelic KT attachments (Cimini *et al.*, 2006; DeLuca *et al.*, 2006; Bakhoun *et al.*, 2009; Thompson *et al.*, 2010). To test whether formation of merotelic KTs was more frequent in cells with incomplete versus complete spindle pole separation, we performed a set of experiments in which GFP- γ -tubulin PtK1 cells were followed by time-lapse microscopy from (or before) NEB until mid prometaphase, at which time the cells were fixed and immunostained for KT and MTs (Figure 3, A and B). The same cells were then relocalized, imaged by high-resolution confocal microscopy, and analyzed to determine the number of merotelic KTs. The mean pole-to-pole distance at NEB in cells with incomplete and complete spindle pole separation was found to be 7.09 ± 2.79 ($N = 19$) and 15.83 ± 3.86 μ m ($N = 36$), respectively, values comparable to those found in the experiments described earlier. Cells with incomplete spindle pole separation at NEB were found to possess significantly (*t* test, $p < 0.01$) higher numbers of merotelic KTs in prometaphase than cells with complete spindle pole separation (Figure 3C). These results

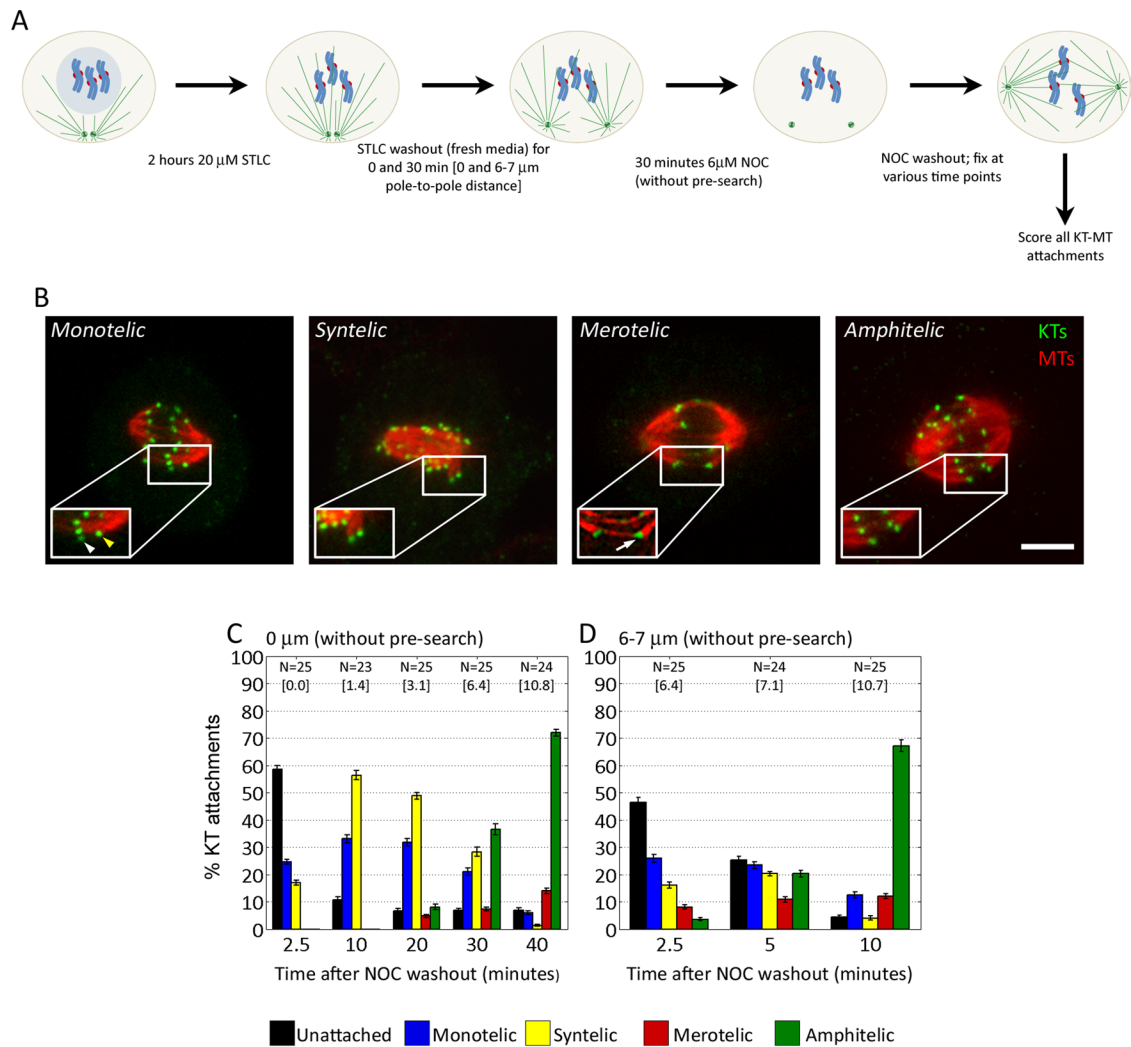


FIGURE 4: Pole-to-pole distance at NEB determines the types and numbers of KT attachments that form in early prometaphase. (A) Flowchart of experimental protocol used for the data summarized in C and D. (B) Examples of different types of KT attachments in PtK1 cells. The images are single focal planes or maximum-intensity projections of two to four optical sections around the chromosome of interest. Insets are 150% enlarged views of the KT or KT pair in the boxed region. White and yellow arrowheads denote the unattached and attached sister KT, respectively. White arrow denotes merotelic KT. Scale bar, 5 μm . (C) Frequencies of different types of KT attachments in cells that were first treated with STLC for 2 h, then washed out and incubated in NOC for 30 min, and finally washed out of the NOC and fixed at subsequent time points. In these cells, the spindle poles started at a distance of 0 μm and gradually separated during MT assembly (spindle poles moving apart from 0 μm without presearch). (D) Frequencies of different types of KT attachments in cells that were first treated with STLC for 2 h, washed out and reincubated in STLC-free media for 30 min (to allow the spindle poles to move apart to a distance of 6–7 μm), then incubated in NOC for 30 min, and finally washed out of the NOC and fixed at subsequent time points. In these cells, the spindle poles started at a distance of 6–7 μm and gradually separated during MT assembly (to mimic incomplete spindle pole separation in untreated PtK1 cells). N, number of cells analyzed for each experimental point. For each cell, the type of KT attachment was determined for all the chromosomes (8.98 ± 1.36 , mean \pm SD) that could be clearly visualized. The numbers in square brackets represent the average pole-to-pole distance (in μm) at each time point.

show that cells in which spindle pole separation is not complete upon NEB, and which thus undergo spindle bipolarization during prometaphase, are more likely to establish KT misattachments than are cells in which spindle pole separation is complete at NEB. Our data also showed that overall the spindle poles were incompletely separated upon NEB in ~45% (N = 122) of our PtK1 cell clone, similar to what was found in HeLa, MCDKII, and PtK2 cells (Rattner and Berns, 1976; Aubin *et al.*, 1980; Whitehead *et al.*, 1996; Rosenblatt *et al.*, 2004; Toso *et al.*, 2009; Woodcock *et al.*, 2010), making these cells a good model in which to study this phenomenon.

Merotelic kinetochore attachments can form through a syntelic intermediate

We next wanted to understand how incomplete spindle pole separation influences the number and types of KT attachments formed and how merotelic attachments arise. To this aim, we experimentally inhibited spindle pole separation by inhibiting the kinesin Eg5 by a 2 h S-trityl-L-cysteine (STLC) treatment (Skoufias *et al.*, 2006). We then washed out the STLC and added nocodazole (NOC) to completely disassemble the MTs. Next we washed out the NOC and fixed the cells at regular time intervals (Figure 4A). Pilot experiments

were performed to identify the minimum dose of NOC and length of treatment that induced MT disassembly but did not result in centrosome displacement or assembly of ectopic sites of MT nucleation after NOC washout. This experimental design allowed spindle pole separation to occur simultaneously with establishment of KT–MT interactions (i.e., search and capture occurs while the spindle poles are moving apart), as would normally happen in untreated cells. Finally, we determined the number and types of KT attachments at different time points until the end of prometaphase (Figure 4, B and C). We found that at early time points there were large numbers of unattached chromosomes and that the attached chromosomes exhibited either syntelic or monotelic attachments (Figure 4C). At later time points, both merotelic and amphitelic attachments increased, whereas syntelic and monotelic decreased (Figure 4C), suggesting that some of the syntelic attachments were converted into merotelic ones. These results suggest that merotelic attachments can form through a syntelic intermediate and that this mechanism may explain the higher frequency of merotelic attachments in cells with incomplete spindle pole separation compared with cells achieving complete centrosome separation before NEB. The types (monotelic and syntelic) of KT attachments (disregarding the unattached chromosomes) at the early time points of our experiment were very similar to those found in cells arrested with Eg5 inhibitors (Kapoor *et al.*, 2000; Khodjakov *et al.*, 2003). Moreover, we performed an experiment in which cells were washed out of STLC after a 2-h treatment, fixed at regular time intervals, and analyzed for numbers and types of KT attachments (initial pole-to-pole distance 0 μm , with pre-search). We found that the changes in numbers and types of KT attachments over time (Supplemental Figure S3A) were very similar to those observed in cells in which spindle pole separation and KT attachment occurred simultaneously (initial pole-to-pole distance 0 μm , without pre-search). Although this experiment was not representative of the events occurring under physiological conditions, it provided useful information for the development of our mathematical model (see later discussion and the Supplemental Material).

Because the pole-to-pole distance upon NEB in untreated cells with incomplete spindle pole separation is never 0 μm , we further modified the experiment. We reincubated the cells in drug-free media between the STLC washout and the NOC treatment to allow enough time for the spindle poles to move apart to a distance of 6–7 μm (Figure 4A), which represents the pole-to-pole distance in untreated cells with incomplete spindle pole separation at NEB (Supplemental Figure S1). We found that an initial pole-to-pole distance of 6–7 μm still resulted in a large number of syntelic chromosomes but overall generated a more random distribution of different types of KT attachments at early time points after NOC washout (see 2.5- and 5-min time points in Figure 4D). It is also noteworthy that in this case, as opposed to when the search starts with spindle poles very close to each other (0- μm distance, Figure 4C), both amphitelic and merotelic attachments formed at early time points, suggesting that merotelic KT misattachments do not necessarily form through a syntelic intermediate. Finally, we also performed the experiment with an initial pole-to-pole distance of 2–3 μm and found that the numbers and types of KT attachments observed at early time points (Supplemental Figure S4) were intermediate between those observed with initial distances of 0 and 6–7 μm . In this case, both amphitelic and merotelic attachments appeared early but at lower frequencies than when the initial distance was 6–7 μm . In all experiments, amphitelic attachments increased over time at the expense of syntelic and monotelic ones, as expected due to attachment of unattached KTs and correction of misattachments. An increase in merotelic attachments was also observed, which may be

due to the conversion of syntelic attachments into merotelic ones due to partial correction of syntelic attachments. Finally, it is also worth noting that in all cases (but particularly for the 0- and 2- to 3- μm pole-to-pole distance) there was an initial increase in the number of syntelic attachments (see Figure 4C, 2.5 and 10 min; Figure 4D, 2.5 and 5 min; and Supplemental Figure S4, 2.5 and 5 min). This suggests not only that when the pole-to-pole distance is small chromosomes tend to establish syntelic attachments, but also that correction of syntelic attachments is not efficient when the spindle poles are not fully separated.

Computational modeling reveals that two spindle poles in close proximity do not search the entire cellular space

To better understand how initial spindle pole distance affects establishment of KT–MT attachments, we took advantage of a computational model we recently developed to simulate spindle assembly in realistic geometry (Paul *et al.*, 2009). We adapted this model to our present experimental system (PtK1 cells) by taking into account a number of parameters, including size of the nuclear space (volume occupied by the chromosomes at NEB), chromosome number, and chromosome size (see the Supplemental Material for information about parameters used in the simulations). We reverse engineered the process of spindle assembly by using the quantitative experimental data described in the preceding section and shown in Figure 4, C and D, and Supplemental Figure S3A. Specifically, we simulated (using the same method as in Paul *et al.*, 2009) the stochastic search for KTs by MTs growing from two poles (Figure 5A), the distance between which was changing as in the three experimental setups (Figure 4, C and D, and Supplemental Figure S3A). In the course of spindle assembly, the monotelically attached chromosomes rotated so that the uncaptured KT became shielded from the capturing pole (Rieder and Alexander, 1990; Nicklas, 1997), thereby decreasing the probability of syntelic and merotelic attachments. Furthermore, the monotelically attached chromosomes moved away from the capturing pole, simulating CENP-E-dependent congression of monotelic chromosomes (Kapoor *et al.*, 2006; Cai *et al.*, 2009), further decreasing the probability of syntelic and merotelic attachment and increasing the chance of amphitelic attachment by the opposing spindle pole. This bias of monotelic chromosomes to move away from the capturing pole increased with increasing pole-to-pole distances, reflecting the increase in number of k-fibers along which the monotelic chromosomes can move (see the Supplemental Material for details). Time-course simulations performed with such a computational model (details in the Supplemental Material) closely reproduced the experimental results for all initial pole-to-pole distances (Figure 5, B and C) and revealed that there are “blind spots” for each of the poles that are maximal when the poles are in close proximity, in which case each pole essentially searches in its own half-space (Figure 5, A and D). Note that these blind spots are not an artificial assumption but are simply the consequence of the steric hindrance that MTs of one centrosome present for MTs growing from the other centrosome when they are in close proximity. As the distance between the poles increases, each pole “sees” increasing fractions of chromosomes, until, when spindle pole separation is complete (~10 μm), almost all chromosomes are seen from both poles (Figure 5D). This “shielding” effect would explain our finding that there is a lag phase in the disappearance (correction) of syntelic attachments in cells with incomplete spindle pole separation (Figures 4, C and D, and Supplemental Figures S3A and S4). Indeed, when the spindle poles are very close to each other a syntelic chromosome would likely only be seen by one pole and therefore would keep forming syntelic attachments even if initially corrected. Finally, the

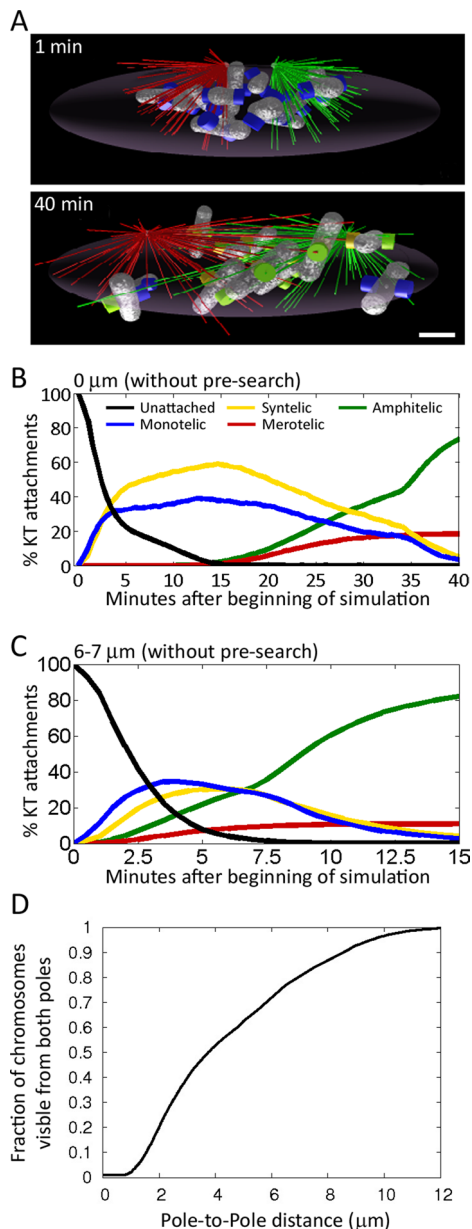


FIGURE 5: Computer simulations of spindle assembly from different initial spindle pole distances can closely reproduce experimental results. (A) Snapshots of computer simulations of spindle assembly in a cell with incomplete spindle pole separation at NEB (top). MTs from different poles are shown in green and red to differentiate between their spindle pole of origin. Unattached KT are blue; captured KT are green. The complete separation of MTs coming from opposite poles in the top image is an exemplification of the “shielding” effect occurring between the two poles when the pole-to-pole distance is very small (see the text for details). (B, C) Time-course simulations of spindle assembly in the presence of a shielding effect between the two centrosomes. (B) Simulation starting with a spindle pole distance of 0 μm (as in Figure 4C). (C) Simulation starting with a spindle pole distance of 6 μm (as in Figure 4D). The simulation results closely reproduce the experimental results both at the initial pole-to-pole distance of 0 μm and at an initial distance of 6 μm. (D) The graph shows the correlation between pole-to-pole distance and the fraction of chromosomes seen from both poles.

mathematical model also explains why merotelic attachments (for which a single KT must be seen by both poles) do not form right away when the spindle poles are in close proximity (Figure 4C and

Supplemental Figure S3A) but start forming at early time points for increasing pole-to-pole distances (Supplemental Figure S4 and Figure 4D). The simulations also demonstrated that MTs attached to syntelic chromosomes have to be unstable, detaching after ~2 min, because otherwise the number of erroneous attachments would be too great. Finally, the model indicates that chromosome rotations and movements toward the spindle equator after the first capture are important for both rapid and accurate spindle assembly.

It is worth noting that the model invoking the shielding effect (Figure 5D) between the two spindle poles could reproduce the experimental results significantly better than alternative models, especially for very small initial pole-to-pole distances. Indeed, a model in which the two poles were allowed to search in the whole space (i.e., no shielding effect; Supplemental Figure S5, A and B) could not reproduce the experimental results in the case of an initial pole-to-pole distance of 0 μm (Supplemental Figure S5A). Specifically, this model resulted in the formation of larger numbers of merotelic KTs at early time points and low numbers of amphitelic KTs at later time points (compare Figure 4C and Supplemental Figure S5A). Results that better fit the experimental data were obtained when the latter model was modified by allowing merotelic and amphitelic KTs to frequently disassemble at small interpolar distances and to become more stable with increasing pole-to-pole distances. Although this modification produced better results (Supplemental Figure S5, C and D), it could not reproduce the changes in frequency of monotelic and syntelic attachments over time for cells starting with an initial pole-to-pole distance of 0 μm (compare Figure 4C and Supplemental Figure S5C).

Finally, we computationally tested additional conditions to account for observations reported in previous studies. Specifically, we varied the inter-KT angle to simulate spindle assembly in the presence of “plastic” KTs (Loncarek *et al.*, 2007), we increased the KT target size to simulate the long k-fibers that form in cells arrested in mitosis by Eg5 inhibition (Khodjakov *et al.*, 2003), and we introduced small unevenness in chromosome distribution. None of these modifications led to better fits of the model results to the experimental data (see the Supplemental Material for details). This does not necessarily mean that the phenomena tested do not play any role in the spindle assembly process, but that they may be more subtle than the other mechanisms/processes considered in this study and/or that the information about dynamic correlations between chromosome and centrosome positions and KT orientations in our hands is insufficient to detect an effect.

DISCUSSION

Incomplete centrosome separation at NEB and kinetochore misattachment

Our data reveal that the degree of centrosome separation upon NEB plays a critical role in determining the number and types of KT attachments that form in early prometaphase. Specifically, we showed that when the centrosomes are not located at opposite ends of the xy-axis of the nuclear space at NEB there is an increase in formation of KT misattachments (Figures 3 and 4, C and D) and consequently an increase in chromosome missegregation (Figures 1 and 2). Our data also indicate that incomplete spindle pole separation at NEB can lead to the formation of merotelic attachments through two different mechanisms (Figure 6): 1) when the spindle poles are very close to each other (<2–3 μm), chromosomes tend to become syntelically attached (Figure 6A). Merotelic attachments will then be formed by partial correction of syntelic attachments during spindle bipolarization (Figure 6A, third and fourth steps). Indeed, our *in silico* data indicate that syntelic attachments are

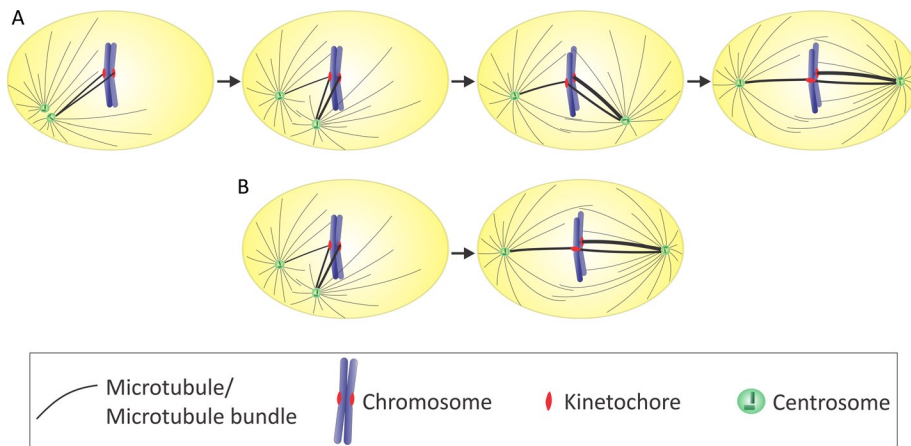


FIGURE 6: Merotelic KT attachments can form through two different mechanisms in cells with incomplete spindle pole separation at NEB. (A) When the spindle poles are very close to each other, chromosomes tend to become syntelically attached. Merotelic attachments will then be formed after partial correction of syntelic attachments during spindle bipolarization (third and fourth steps). (B) If the spindle poles are incompletely separated but far enough from each other, a single KT can be seen by and establish attachment with both spindle poles right away, without going through a syntelic intermediate.

much more unstable than merotelic and amphitelic ones. This suggests that, *in vivo*, syntelic attachments may be corrected more efficiently than merotelic ones, as previously suggested by others (Khodjakov and Rieder, 2009; Nezi and Musacchio, 2009; Yang *et al.*, 2009). Such an efficient correction may in turn explain why merotelic attachments are observed much more frequently than syntelic ones in tissue culture cells (Hauf *et al.*, 2003; Cimini, 2008). Efficient correction of syntelic attachments may also be required for spindle bipolarization. Indeed, if Aurora B kinase is inhibited in PtK1 cells recovering from an STLC arrest, both correction of syntelic attachments and bipolarization are inhibited/delayed in most cells (W. T. Silkworth, I. K. Nardi, and D. Cimini, unpublished results). 2) If the spindle poles are incompletely separated upon NEB but far enough from each other ($\geq 2\text{--}3\ \mu\text{m}$), then merotelic attachments can also form through a second mechanism (Figure 6B), in which a single KT would be seen by and establish attachment with both spindle poles directly, without going through a syntelic intermediate. Of interest, even though a certain degree of centrosome separation ($6\text{--}7\ \mu\text{m}$) is always achieved before NEB, in many cells ($\sim 45\%$) this separation does not reach the maximum possible distance. Such partial spindle pole separation is enough to increase the rate of KT misattachment formation and chromosome missegregation compared with cells exhibiting complete spindle pole separation ($>10\ \mu\text{m}$) at NEB (Figures 1 and 2).

Prophase versus prometaphase centrosome separation

As described here and in other studies (Rattner and Berns, 1976; Aubin *et al.*, 1980; Whitehead *et al.*, 1996; Kapoor *et al.*, 2000; Rosenblatt *et al.*, 2004; Kaseda *et al.*, 2009b; Toso *et al.*, 2009), spindle length and/or structure at the end of prometaphase are not affected by the position of the centrosomes at NEB because centrosome separation can be completed after NEB. It has been proposed that there is substantial redundancy during bipolar spindle assembly aimed at ensuring accurate chromosome segregation (Rosenblatt, 2005; Tanenbaum and Medema, 2010), and the existence of mechanisms that allow completion of centrosome separation either in prophase or in prometaphase was believed to exemplify such redundancy (Whitehead *et al.*, 1996; Kaseda *et al.*, 2009a; Toso *et al.*, 2009). However, we show here that, although cells in

which centrosome separation is not completed before NEB do not exhibit permanent defects of spindle organization or structure, they do exhibit increased rates of chromosome missegregation compared with cells in which centrosome separation is completed before NEB. Thus the mechanisms responsible for prometaphase centrosome separation may represent a backup system that ensures progression of mitosis in spite of the potential risk. Of interest, during the early stages of embryonic development, the spindle poles are completely separated at NEB (Robinson *et al.*, 1999; Rosenblatt, 2005), indicating that prophase centrosome separation is highly prevalent in this context. It is likely that the completion of centrosome separation before NEB at this stage of development ensures the accuracy of chromosome segregation required for development of a healthy adult organism. Similarly, RPE1 cells, known for maintaining a stable diploid chromosome number,

were found to achieve complete centrosome separation prior to NEB 100% of the time (Magidson *et al.*, 2011).

Although traditionally the existence of two different pathways has been invoked to explain how centrosome separation can be completed either before or after NEB, our data on the pole-to-pole distance upon NEB (Supplemental Figure S2) do not seem to support a two-pathway model. Indeed, if centrosome separation occurred through one of two alternative pathways, one would expect to find a bimodal distribution of pole-to-pole distances at NEB. Instead, we found a continuous distribution of distances upon NEB, suggesting that there are not two distinct pathways, but rather a number of mechanisms, some of which can be used in prophase (MT/nuclear envelope interaction), some in prometaphase (myosin activity at the cell cortex), and some in both (Eg5-dependent MT sliding). Nevertheless, it does appear that at least in some cell types centrosome separation and NEB are sufficiently uncoordinated that the number of cells in which centrosome separation is incomplete at NEB is relatively high (Rattner and Berns, 1976; Aubin *et al.*, 1980; Waters *et al.*, 1993; Whitehead *et al.*, 1996; Rosenblatt *et al.*, 2004; Toso *et al.*, 2009). At this time we have only limited information on how prevalent incomplete centrosome separation at NEB is in different cell types. However, we have preliminary data showing that in several different cancer cell lines a large proportion of cells exhibit incomplete centrosome separation in early mitosis (W. T. Silkworth, I. K. Nardi, and D. Cimini, unpublished results). Thus it is possible that under normal conditions (e.g., early development and untransformed or primary cells) there would be a selective pressure against delayed centrosome separation due to its association with chromosome missegregation and aneuploidy, which may, in turn, reduce cell viability. However, situations in which there are high proliferation rates and misregulation of many physiological pathways, as in cancer cells, centrosomes may fail to achieve complete separation before NEB much more frequently. Of interest, incomplete spindle pole separation in cancer cells may represent a mechanism associated with chromosomal instability in addition to previously identified ones, such as transient spindle multipolarity (Ganem *et al.*, 2009; Silkworth *et al.*, 2009) and inefficient correction of KT misattachments (Bakhoun *et al.*, 2009).

Why does incomplete spindle pole separation at NEB induce kinetochore misattachments and chromosome missegregation?

The work presented here indicates that if the centrosomes are not in diametrically opposed positions along the *xy*-axis of the nuclear space at the time of NEB, KTs are likely to establish erroneous attachments (Figures 3–5). A consequence of the high rates of misattachment formation is chromosome missegregation at later mitotic stages (Figures 1 and 2). Specifically, high rates of merotelic KT formation are expected to result in high rates of chromosome missegregation (Cimini *et al.*, 2003b; Ganem *et al.*, 2009; Silkworth *et al.*, 2009) because merotelic KT attachments are not detected by the spindle assembly checkpoint (Khodjakov *et al.*, 1997a; Wise and Brinkley, 1997; Yu and Dawe, 2000; Cimini *et al.*, 2002, 2004). Over the years, several different factors have been shown to promote KT misattachments (in particular merotelic). These include altered centromere/chromosome architecture (Stear and Roth, 2002; Cimini *et al.*, 2003a; Gregan *et al.*, 2007; Samoshkin *et al.*, 2009; Manning *et al.*, 2010) and defects in mitotic spindle morphology/assembly (Heneen, 1975; Sluder *et al.*, 1997; Ganem *et al.*, 2009; Paul *et al.*, 2009; Silkworth *et al.*, 2009). In this study, we show that a delay in spindle bipolarization also leads to increased rates of merotelic KT formation (Figures 3–5). Specifically, both our experimental and computational data show that cells with incomplete spindle pole separation upon NEB establish a large number (20–60%) of syntelic attachments (Figures 3 and 4 and Supplemental Figure S4). However, our data suggest that it is not the prometaphase bipolarization per se that induces KT misattachment but rather the relative positions of the two centrosomes/spindle poles at the time of NEB with respect to the nuclear space. In fact, if the two spindle poles are not completely separated upon NEB, the early prometaphase spindle will be skewed and/or will have spindle poles positioned very close to each other. In two types of centrosome positioning configurations (Figure 1B, iii and iv) we observed both a reduced pole-to-pole distance and a skewed placement of the centrosomes toward one-half of the nuclear space. In a third type, initially separated centrosomes (Figure 1A, ii) moved to the center of the nuclear space upon NEB (Figure 1B, ii), which resulted in a symmetrical configuration but in very short pole-to-pole distance. This behavior was observed in only a small number of cells (<5% of the overall mitotic cell population), and it appears to exemplify a difference between PtK1 cells and several human cell types. Indeed, it was previously shown that in human cells the centrosomes can reach diametrically opposing positions along the *z*-axis before NEB. As opposed to what we observe in PtK1 cells, in human cells the centrosomes persist in those positions after NEB, and the spindle assembles perpendicular to the substrate (Chaly and Brown, 1988; Mosgoller *et al.*, 1991; Nagele *et al.*, 1995; Magidson *et al.*, 2011). This results in the chromosomes at the metaphase plate frequently appearing in what is known as a wheel-shaped rosette (Nagele *et al.*, 1995) or the toroidal configuration (Magidson *et al.*, 2011). In our cells, when the centrosomes are positioned along the *z*-axis prior to NEB, they move toward the center of the nuclear space upon NEB (Figure 1, A and B, ii, and Supplemental Figure S1A), thus preventing spindle assembly perpendicular to the substrate. As a result, we never observed metaphase PtK1 cells with chromosomes in a rosette configuration. Thus, in human cells prophase centrosome separation along the *z*-axis is not expected to affect KT attachment or chromosome segregation (Magidson *et al.*, 2011). Conversely, in PtK1 cells centrosome separation along the *z*-axis is not maintained upon NEB, and therefore it results in short pole-to-pole distances upon NEB, which are associated with KT misattachment and chromosome missegregation (this

study). In summary, we find that incomplete centrosome separation upon NEB can result in asymmetrical positioning of the spindle poles with respect to the nuclear space at the onset of prometaphase and in all cases is characterized by a short pole-to-pole distance. As indicated by our mathematical model, the two spindle poles can only see a fraction of the chromosomes at short pole-to-pole distances (Figure 5D), and this gives rise to large numbers of KT misattachments.

Recent studies showed that transient spindle multipolarity promotes formation of merotelic attachments in cancer cells (Ganem *et al.*, 2009; Paul *et al.*, 2009; Silkworth *et al.*, 2009). Like transient multipolarity, incomplete spindle pole separation upon NEB leads to a temporary geometric defect of the mitotic spindle. However, although both situations will result in elevated rates of chromosome missegregation, they are mechanistically very different. In the case of a cell with two unseparated centrosomes, each chromosome can likely be seen by only one centrosome, and this results in high frequencies of syntelic attachments. Conversely, within a multipolar spindle each chromosome is likely seen by more than one centrosome, favoring merotelic attachment over syntelic.

MATERIALS AND METHODS

Cell culture and drug treatments

Both PtK1 cells (a generous gift from Ted Salmon, University of North Carolina, Chapel Hill, NC) and PtK-GFP- γ -tubulin (a generous gift from Alexey Khodjakov, Wadsworth Center, Albany, NY) were maintained in Ham's F-12 medium (Life Technologies, Carlsbad, CA). The culture medium was supplemented with 10% fetal bovine serum, penicillin, streptomycin, and amphotericin B (antimycotic). Cells were grown in a 37°C, 5% CO₂, humidified incubator. For experiments, cells were grown on sterile coverslips inside 35-mm Petri dishes. Cells at ~80% confluency were incubated in media containing 20 μ M STLC for 2 h and either fixed (0 μ m with presearch) or washed out of the drug. STLC washout was performed by washing the cells in fresh media four times. After washout, cells were either immediately incubated in media containing 6 μ M NOC for 30 min (0 μ m without presearch) or reincubated in drug-free media for 15 min (2–3 μ m without presearch) or 30 min (6–7 μ m without presearch) before the NOC treatment. NOC was then washed out, and cells were either fixed immediately (2.5 min) or reincubated in drug-free media and fixed at regular time intervals.

Fixation and immunostaining

Cells were rapidly rinsed in 1 \times PHEM buffer (60 mM PIPES, 25 mM HEPES, 10 mM EGTA, 2 mM MgCl₂) and incubated in ice-cold 95% methanol with 5 mM ethylene glycol tetraacetic acid for 5 min first and then again for 20 min at –20°C. Subsequently, cells were washed in phosphate-buffered saline (PBS) and then blocked in 10% boiled goat serum for 1 h at room temperature. The coverslips were then incubated overnight at 4°C in primary antibodies diluted in 5% boiled goat serum. Cells were finally washed in PBST (PBS with 0.05% Tween 20), incubated in secondary antibodies diluted in 5% boiled goat serum for 1 h at room temperature, washed again, stained with 4',6-diamidino-2-phenylindole, and mounted in an antifade solution containing 90% glycerol and 0.5% *N*-propyl gallate. Primary antibodies were diluted as follows: human anticentromere antigen (Antibodies Incorporated, Davis, CA), diluted 1:100; mouse anti- α -tubulin (DM1A; Sigma-Aldrich, St. Louis, MO), diluted 1:500. Secondary antibodies were diluted as follows: X-rhodamine goat anti-human (Jackson ImmunoResearch Laboratories, West Grove, PA), diluted 1:100; and Alexa 488 goat anti-mouse (Molecular Probes, Invitrogen, Carlsbad, CA), diluted 1:400.

Live-cell imaging

Ptk1 cells expressing GFP- γ -tubulin were grown on coverslips to ~70% confluency and mounted into a Rose chamber (Rieder and Hard, 1990) with a top coverslip. The chamber was injected with L-15 medium supplemented with 4.5 g/l glucose. Experiments were performed on a Nikon (Melville, NY) Eclipse Ti inverted microscope equipped with phase-contrast transillumination, transmitted light shutter, Lumen 200PRO fluorescence illumination system, ProScan automated stage (Prior Scientific, Rockland, MA), and HQ2 CCD camera (Photometrics, Tucson, AZ). Cells were maintained at ~36°C by means of an Air Stream stage incubator (Nevtek, Williamsville, VA). Image acquisition, shutters, z-axis position, and Lumen 200PRO fluorescence illumination system were all controlled by NIS Elements AR software (Nikon) on a PC. To determine the time of NEB, the cells were monitored by phase contrast every 1–2 min, whereas simultaneous phase contrast and fluorescence images were acquired at a single focal plane every 3 min for a 1- to 2-h period with a Plan Apochromatic 60 \times , 1.4-numerical aperture (NA) phase-contrast objective. Extra images were acquired immediately following NEB, at which time the positions of the centrosomes were also recorded. To record the centrosome coordinates prior to and upon NEB, the experiment was manually switched from time-lapse to live imaging, the centrosome positions were identified by focusing up and down along the z-axis, and the coordinates were recorded. Time-lapse imaging was then resumed. To further confirm centrosome positioning and pole-to-pole distances, an additional set of cells with incomplete spindle pole separation was imaged by four-dimensional (three-dimensional plus time) microscopy. For these cells, z-series optical sections were obtained in seven 1.2- μ m steps using a Plan Apochromatic 60 \times , 1.4-NA phase-contrast objective. After completion of spindle pole separation, images were acquired at a single focal plane to follow the cells into anaphase. The collected images were subsequently analyzed to 1) determine centrosome positions with respect to the nuclear space, 2) measure pole-to-pole distances before and upon NEB, and 3) determine the chromosome segregation phenotype. For relocalization experiments, cells were grown on coverslips photoetched with an alphanumeric grid pattern (Electron Microscopy Sciences, Hatfield, PA) and imaged until mid prometaphase (~10 min after NEB), at which time the specific alphanumeric grid was recorded, and the cells were removed from the microscope and immediately fixed and immunostained as described. After immunostaining, cells were relocalized (using previously recorded alphanumeric grid), imaged, and analyzed as described in the following section.

Confocal microscopy and image analysis

Immunofluorescently stained cells were imaged with a Swept Field Confocal system (Prairie Technologies, Middleton, WI) on a Nikon Eclipse TE-2000U inverted microscope. The microscope was equipped with a 100 \times , 1.4-NA Plan Apochromatic phase-contrast objective lens, phase-contrast transillumination, transmitted light shutter, and automated ProScan stage (Prior Scientific). The confocal head was equipped with filters for illumination at 488, 568, and 647 nm from a 400-mW argon laser and a 150-mW krypton laser. Digital images were acquired with an HQ2 CCD camera (Photometrics). Image acquisition, shutter, z-axis position, laser lines, and confocal system were all controlled by NIS Elements AR software (Nikon) on a PC. The z-series optical sections through each cell analyzed were obtained at 0.6- μ m steps. For determination of the numbers of merotelic KTs in relocalized cells and unattached, monotelic, amphitelic, syntelic, and merotelic attachments in the fixed-cell time-course experiments, acquired images were analyzed as previously described (Silkworth *et al.*, 2009).

ACKNOWLEDGMENTS

We thank Alexey Khodjakov for providing the Ptk-GFP- γ -tubulin cells. We thank the members of the Cimini lab for helpful discussion. I.K.N. was a recipient of a Fralin Summer Undergraduate Research Fellowship and an Atlantic Coast Conference Undergraduate Research Scholars Award. This work was supported by National Science Foundation Grant MCB-0842551 to D.C. and National Institutes of Health Grant GM068952 to A.M.

REFERENCES

- Aubin JE, Osborn M, Weber K (1980). Variations in the distribution and migration of centriole duplexes in mitotic Ptk2 cells studied by immunofluorescence microscopy. *J Cell Sci* 43, 177–194.
- Bakhoun SF, Genovese G, Compton DA (2009). Deviant kinetochore microtubule dynamics underlie chromosomal instability. *Curr Biol* 19, 1937–1942.
- Brinkley BR, Cartwright J Jr (1971). Ultrastructural analysis of mitotic spindle elongation in mammalian cells in vitro. Direct microtubule counts. *J Cell Biol* 50, 416–431.
- Cai S, O'Connell CB, Khodjakov A, Walczak CE (2009). Chromosome congression in the absence of kinetochore fibres. *Nat Cell Biol* 11, 832–838.
- Cameron LA, Yang G, Cimini D, Canman JC, Kisurina-Evgenieva O, Khodjakov A, Danuser G, Salmon ED (2006). Kinesin 5-independent poleward flux of kinetochore microtubules in Ptk1 cells. *J Cell Biol* 173, 173–179.
- Chaly N, Brown DL (1988). The prometaphase configuration and chromosome order in early mitosis. *J Cell Sci* 91 (Pt 3), 325–335.
- Cimini D (2008). Merotelic kinetochore orientation, aneuploidy, and cancer. *Biochim Biophys Acta* 1786, 32–40.
- Cimini D, Cameron LA, Salmon ED (2004). Anaphase spindle mechanics prevent mis-segregation of merotelically oriented chromosomes. *Curr Biol* 14, 2149–2155.
- Cimini D, Fioravanti D, Salmon ED, Degraffi F (2002). Merotelic kinetochore orientation versus chromosome mono-orientation in the origin of lagging chromosomes in human primary cells. *J Cell Sci* 115, 507–515.
- Cimini D, Howell B, Maddox P, Khodjakov A, Degraffi F, Salmon ED (2001). Merotelic kinetochore orientation is a major mechanism of aneuploidy in mitotic mammalian tissue cells. *J Cell Biol* 153, 517–527.
- Cimini D, Mattiuzzo M, Torosantucci L, Degraffi F (2003a). Histone hyperacetylation in mitosis prevents sister chromatid separation and produces chromosome segregation defects. *Mol Biol Cell* 14, 3821–3833.
- Cimini D, Moree B, Canman JC, Salmon ED (2003b). Merotelic kinetochore orientation occurs frequently during early mitosis in mammalian tissue cells and error correction is achieved by two different mechanisms. *J Cell Sci* 116, 4213–4225.
- Cimini D, Wan X, Hirel CB, Salmon ED (2006). Aurora kinase promotes turnover of kinetochore microtubules to reduce chromosome segregation errors. *Curr Biol* 16, 1711–1718.
- DeLuca JG, Gall WE, Ciferri C, Cimini D, Musacchio A, Salmon ED (2006). Kinetochore microtubule dynamics and attachment stability are regulated by Hec1. *Cell* 127, 969–982.
- Ganem NJ, Godinho SA, Pellman D (2009). A mechanism linking extra centrosomes to chromosomal instability. *Nature* 460, 278–282.
- Gonczy P, Pichler S, Kirkham M, Hyman AA (1999). Cytoplasmic dynein is required for distinct aspects of MTOC positioning, including centrosome separation, in the one cell stage *Caenorhabditis elegans* embryo. *J Cell Biol* 147, 135–150.
- Gregan J, Riedel CG, Pidoux AL, Katou Y, Rumpf C, Schleiffer A, Kearsey SE, Shirahige K, Allshire RC, Nasmyth K (2007). The kinetochore proteins Pcs1 and Mde4 and heterochromatin are required to prevent merotelic orientation. *Curr Biol* 17, 1190–1200.
- Hauf S, Cole RW, LaTerra S, Zimmer C, Schnapp G, Walter R, Heckel A, van Meel J, Rieder CL, Peters JM (2003). The small molecule hesperadin reveals a role for Aurora B in correcting kinetochore-microtubule attachment and in maintaining the spindle assembly checkpoint. *J Cell Biol* 161, 281–294.
- Heneen WK (1975). Kinetochores and microtubules in multipolar mitosis and chromosome orientation. *Exp Cell Res* 91, 57–62.
- Kapoor TM, Lampson MA, Hergert P, Cameron L, Cimini D, Salmon ED, McEwen BF, Khodjakov A (2006). Chromosomes can congress to the metaphase plate before biorientation. *Science* 311, 388–391.
- Kapoor TM, Mayer TU, Coughlin ML, Mitchison TJ (2000). Probing spindle assembly mechanisms with monastrol, a small molecule inhibitor of the mitotic kinesin, Eg5. *J Cell Biol* 150, 975–988.

- Kasada K, McAinsh A, Cross RA (2009a). A countdown clock in mitotic prophase: design logic for dual pathway mitosis. Presented at American Society for Cell Biology 2009 meeting, 5–9 December 2009. Available at: <http://f1000.com/posters/browse/summary/100> (accessed 4 January 2012).
- Kasada K, McAinsh AD, Cross RA (2009b). Walking, hopping, diffusing and braking modes of kinesin-5. *Biochem Soc Trans* 37, 1045–1049.
- Khodjakov A, Cole RW, McEwen BF, Buttle KF, Rieder CL (1997a). Chromosome fragments possessing only one kinetochore can congress to the spindle equator. *J Cell Biol* 136, 229–240.
- Khodjakov A, Cole RW, Rieder CL (1997b). A synergy of technologies: combining laser microsurgery with green fluorescent protein tagging. *Cell Motil Cytoskeleton* 38, 311–317.
- Khodjakov A, Copenagle L, Gordon MB, Compton DA, Kapoor TM (2003). Minus-end capture of preformed kinetochore fibers contributes to spindle morphogenesis. *J Cell Biol* 160, 671–683.
- Khodjakov A, Rieder CL (2009). The nature of cell-cycle checkpoints: facts and fallacies. *J Biol* 8, 88.
- Kline-Smith SL, Khodjakov A, Hergert P, Walczak CE (2004). Depletion of centromeric MCAK leads to chromosome congression and segregation defects due to improper kinetochore attachments. *Mol Biol Cell* 15, 1146–1159.
- Loncerek J, Kisurina-Evgenieva O, Vinogradova T, Hergert P, La Terra S, Kapoor TM, Khodjakov A (2007). The centromere geometry essential for keeping mitosis error free is controlled by spindle forces. *Nature* 450, 745–749.
- Magidson V, O'Connell CB, Loncerek J, Paul R, Mogilner A, Khodjakov A (2011). The spatial arrangement of chromosomes during prometaphase facilitates spindle assembly. *Cell* 146, 555–567.
- Manning AL, Longworth MS, Dyson NJ (2010). Loss of pRB causes centromere dysfunction and chromosomal instability. *Genes Dev* 24, 1364–1376.
- Mole Bajer J (1975). The role of centrioles in the development of the astral spindle (newt). *Cytobios* 13, 117–140.
- Mosgoller W, Leitch AR, Brown JK, Heslop-Harrison JS (1991). Chromosome arrangements in human fibroblasts at mitosis. *Hum Genet* 88, 27–33.
- Nagele R, Freeman T, McMorrow L, Lee HY (1995). Precise spatial positioning of chromosomes during prometaphase: evidence for chromosomal order. *Science* 270, 1831–1835.
- Nezi L, Musacchio A (2009). Sister chromatid tension and the spindle assembly checkpoint. *Curr Opin Cell Biol* 21, 785–795.
- Nicklas RB (1997). How cells get the right chromosomes. *Science* 275, 632–637.
- Paul R, Wollman R, Silkworth WT, Nardi IK, Cimini D, Mogilner A (2009). Computer simulations predict that chromosome movements and rotations accelerate mitotic spindle assembly without compromising accuracy. *Proc Natl Acad Sci U S A* 106, 15708–15713.
- Rattner JB, Berns MW (1976). Centriole behavior in early mitosis of rat kangaroo cells (PTK2). *Chromosoma* 54, 387–395.
- Rieder CL, Alexander SP (1990). Kinetochores are transported poleward along a single astral microtubule during chromosome attachment to the spindle in newt lung cells. *J Cell Biol* 110, 81–95.
- Rieder CL, Hard R (1990). Newt lung epithelial cells: cultivation, use, and advantages for biomedical research. *Int Rev Cytol* 122, 153–220.
- Robinson JT, Wojcik EJ, Sanders MA, McGrail M, Hays TS (1999). Cytoplasmic dynein is required for the nuclear attachment and migration of centrosomes during mitosis in *Drosophila*. *J Cell Biol* 146, 597–608.
- Rosenblatt J (2005). Spindle assembly: asters part their separate ways. *Nat Cell Biol* 7, 219–222.
- Rosenblatt J, Cramer LP, Baum B, McGee KM (2004). Myosin II-dependent cortical movement is required for centrosome separation and positioning during mitotic spindle assembly. *Cell* 117, 361–372.
- Salmon ED, Cimini D, Cameron LA, DeLuca JG (2005). Merotelic kinetochores in mammalian tissue cells. *Philos Trans R Soc Lond B Biol Sci* 360, 553–568.
- Samoshkin A, Arnautov A, Jansen LE, Ouspenski I, Dye L, Karpova T, McNally J, Dasso M, Cleveland DW, Strunnikov A (2009). Human condensin function is essential for centromeric chromatin assembly and proper sister kinetochore orientation. *PLoS ONE* 4, e6831.
- Sharp DJ, Yu KR, Sisson JC, Sullivan W, Scholey JM (1999). Antagonistic microtubule-sliding motors position mitotic centrosomes in *Drosophila* early embryos. *Nat Cell Biol* 1, 51–54.
- Silkworth WT, Nardi IK, Scholl LM, Cimini D (2009). Multipolar spindle pole coalescence is a major source of kinetochore mis-attachment and chromosome mis-segregation in cancer cells. *PLoS ONE* 4, e6564.
- Skoufias DA, DeBonis S, Saoudi Y, Lebeau L, Crevel I, Cross R, Wade RH, Hackney D, Kozielski F (2006). S-trityl-L-cysteine is a reversible, tight binding inhibitor of the human kinesin Eg5 that specifically blocks mitotic progression. *J Biol Chem* 281, 17559–17569.
- Sluder G, Thompson EA, Miller FJ, Hayes J, Rieder CL (1997). The checkpoint control for anaphase onset does not monitor excess numbers of spindle poles or bipolar spindle symmetry. *J Cell Sci* 110, 421–429.
- Stear JH, Roth MB (2002). Characterization of HCP-6, a *C. elegans* protein required to prevent chromosome twisting and merotelic attachment. *Genes Dev* 16, 1498–1508.
- Tanenbaum ME, Macurek L, Galjart N, Medema RH (2008). Dynein, Lis1 and CLIP-170 counteract Eg5-dependent centrosome separation during bipolar spindle assembly. *EMBO J* 27, 3235–3245.
- Tanenbaum ME, Medema RH (2010). Mechanisms of centrosome separation and bipolar spindle assembly. *Dev Cell* 19, 797–806.
- Thompson SL, Bakhom SF, Compton DA (2010). Mechanisms of chromosomal instability. *Curr Biol* 20, R285–R295.
- Toso A, Winter JR, Garrod AJ, Amaro AC, Meraldi P, McAinsh AD (2009). Kinetochore-generated pushing forces separate centrosomes during bipolar spindle assembly. *J Cell Biol* 184, 365–372.
- Waters JC, Cole RW, Rieder CL (1993). The force-producing mechanism for centrosome separation during spindle formation in vertebrates is intrinsic to each aster. *J Cell Biol* 122, 361–372.
- Whitehead CM, Rattner JB (1998). Expanding the role of HsEg5 within the mitotic and post-mitotic phases of the cell cycle. *J Cell Sci* 111 (Pt 17), 2551–2561.
- Whitehead CM, Winkfein RJ, Rattner JB (1996). The relationship of HsEg5 and the actin cytoskeleton to centrosome separation. *Cell Motil Cytoskeleton* 35, 298–308.
- Wise DA, Brinkley BR (1997). Mitosis in cells with unreplicated genomes (MUGs): spindle assembly and behavior of centromere fragments. *Cell Motil Cytoskeleton* 36, 291–302.
- Woodcock SA, Rushton HJ, Castaneda-Saucedo E, Myant K, White GR, Blyth K, Sansom OJ, Malliri A (2010). Tiam1-Rac signaling counteracts Eg5 during bipolar spindle assembly to facilitate chromosome congression. *Curr Biol* 20, 669–675.
- Yang Z, Kenny AE, Brito DA, Rieder CL (2009). Cells satisfy the mitotic checkpoint in Taxol, and do so faster in concentrations that stabilize syntelic attachments. *J Cell Biol* 186, 675–684.
- Yu HG, Dawe RK (2000). Functional redundancy in the maize meiotic kinetochore. *J Cell Biol* 151, 131–142.

Supplemental material

Timing of centrosome separation is important for accurate chromosome segregation.

William T. Silkworth*, Isaac K. Nardi*§, Raja Paul†, Alex Mogilner‡, and Daniela Cimini*

* Department of Biological Sciences, Virginia Tech, 1981 Kraft Dr., Blacksburg, VA, 24061, USA

† Indian Association for the Cultivation of Science, Jadavpur, Kolkata 700032, India

‡ Department of Neurobiology, Physiology and Behavior and Department of Mathematics, University of California, Davis, CA 95616, USA

§ Current address: Department of Molecular Cell and Developmental Biology, University of Virginia, School of Medicine, Charlottesville VA 22908, USA

Running Head: Centrosome separation and missegregation

Corresponding author:

Daniela Cimini

Virginia Tech, Dept. Biological Sciences

1981 Kraft Dr.

Blacksburg, VA, 24061 – USA

Tel. ++1-540-231-3922

Fax ++1-540 -231-3414

e-mail: cimini@vt.edu

Development of a mathematical model for simulation of spindle assembly in PtK1 cells.

Approximate kinetics of spindle assembly. We recently considered an extremely simplified model (Mogilner and Craig, 2010) of microtubules (MTs) from two poles searching for a single chromosome equidistant from the poles. In the model, the MTs capture one of two kinetochores (KTs) with the rate k_{on} and the pole-KT connection is destabilized with the rate k_{off} . Thus, all pole-KT connections are transient, except for the amphitelic connection, which was assumed to be stable. We found, not surprisingly, that numbers of mono-, syn- and mero-telic attachments in this model increased at first, and then slowly decreased to zero, while the number of amphitelic connections increased monotonically to saturation.

Simulations of this model suggested starting with a numerical investigation of an approximate temporal dynamics of the spindle assembly to develop intuition without complications of the explicit spatial chromosome distribution. We will call the assembly of the spindle when the poles are initially very close to each other and the search takes place for 1-2 hours before pole separation **Experiment 1** (Figure S3A); the assembly when the poles are initially very close to each other and the search starts together with pole separation **Experiment 2** (Figure 4C); and finally the assembly when the poles start separating from the initial distance 6-7 μm together with the search **Experiment 3** (Figure 4D).

Experiment 1 informs that after 1-2 hours of search, most KT's are associated with MTs and that at pole separation onset there are almost no unattached, mero- and amphi-telic connections present. If MTs from each pole grow in all directions, then each KT is 'seen' from almost the same angle from both poles because in this experiment the poles are so close together.

In this scenario, there is an equal probability to capture any KT from either pole. Thus, in theory, if one KT is captured from one pole, there is an equal chance that the sister KT would be captured from the same as from the other pole. This argument suggests that at early time points following pole separation onset there would be a large number of merotelic and amphitelic attachments in addition to syntelic ones, which was not the case in the experimental results (Figure 4C). One of the most straightforward solutions for this conundrum is that when the centrosomes are very close together, then each searches in its own half-space (Figure 5A), so that each chromosome can only be captured from one of the poles. One possible explanation is that if the poles are close together, MTs from each pole can only cover a half-space because each pole ‘shields’ the other half-space from the other pole.

Furthermore, the data from Experiment 1 indicate clearly that MTs have to detach from the syntelically attached KTs. The respective MT detachment rate cannot be as fast as $\sim 1/\text{minute}$ because in that case the attachment rate would have to be of the same order of magnitude, and the spindle would assemble within a couple of minutes, which does not happen. On the other hand, the detachment rate cannot be slower than $\sim 1/30 \text{ min}$ – in this case, the syntelic attachments would not have time to disassemble in all experiments. Thus, the detachment rate (conversion of syntelic to monotelic attachments) is of the order of one per 10-20 min. This means that during the initial 1-2 hrs, the numbers of syn- and mono-telic attachments equilibrate. Let N_1 and N_2 be the numbers of mono- and syntelic attachments, respectively, k_1 is the rate of monotelic attachment conversion into a syntelic one, and k_2 - the rate of syntelic attachment conversion into a monotelic one (Figure S6). Then, $k_1 N_1 = k_2 N_2$. From the data at $t = 0$ in Experiment 1, $2N_1 \approx N_2$,

so $k_1 = 2k_2$: if $k_2 = 0.05/\text{min}$, then $k_1 = 0.1/\text{min}$. The complete spindle assembly time, about 15 min, scales as the logarithms of the KT number (Mogilner and Craig, 2010), so this time is of the order of $(1/k_0)\log 24 \sim 15 \text{ min}$, where k_0 is the rate of the capture of one KT. Thus, we can estimate the rate of the capture of one KT as $k_0 = \log 24/15 = 0.2/\text{min}$.

All three experiments (Figures S3A, 4C-D) show only increase of mero- and amphitelic connections over time. To account for this, we assumed that amphitelic and merotelic attachments do not disassemble. Although this is a simplification because correction of merotelic attachments is known to occur (Cimini, 2007), mathematical models that predict the observed results but that also include disassembly of merotelic KT attachments are too complex, and were not considered.

Based on these arguments, we screened the parameters and found that if we assume that a monotelic attachment is established with the rate 0.3/min, syntelic one is established with the rate 0.6/min, destabilization rate of the syntelic attachment is 0.3/min, rate of merotelic attachment formation (from mono- or syntelic one) is 0.03/min, and finally if the rate of amphitelic attachment formation from the monotelic one is 0.15/min, we can semi-quantitatively explain the data of all three experiments. In addition to these rates, we also have to assume that the following fraction of chromosomes is *visible from both poles* as a function of the pole-to-pole distance: $f(r) = r^n / (r^n + s^n)$, $n = 4$, $s = 5 \mu\text{m}$. (Here r is the pole-to-pole distance in μm). Based on this function, each pole can access only half of the chromosomes for a pole-to-pole distance of up to 2 μm ; between 2 and 8 μm pole-to-pole distance, the fraction of chromosomes that both poles

can reach linearly increases so that at 5 μm half of the chromosomes can be captured from both poles; and above 8 μm , almost all chromosomes are visible from both poles (Figure 5D).

Simulation of spindle assembly kinetics using the model described above explains the data of the beginning of experiment 1, and then it semi-quantitatively predicts that as the poles separate in this experiment and more chromosomes can be reached from both poles, the initially high monotelic and syntelic numbers decrease because stable amphitelic and merotelic attachments emerge. In experiments 2 and 3, this simple model predicts correctly that mono- and syntelic connection numbers increase in the first ~ 10 min, and then decrease. However, quantitative fits of the model predictions to the data are impossible for such a simple model. Specifically, very rapid increase of the amphitelic attachment number at the end of the search, as well as rapid increase of the merotelic attachment number at the beginning of the search are hard to capture numerically. In addition, the attachment rates that are constant in this model have to depend on actual location of the chromosomes in space. In order to reverse-engineer the data of the three experiments, we undertook the spatially explicit simulations described below.

Spatially explicit simulations. We considered the nuclear space to be an oblate spheroid with dimensions $19 \mu\text{m} \times 19 \mu\text{m} \times 5 \mu\text{m}$ (based on experimentally measured dimensions), with 12 chromosomes (24 kinetochores) inside and 2 centrosomes at the periphery. Chromosomes and KTs were cylindrical objects with dimensions given below. During the search, each centrosome nucleated 100 MTs undergoing dynamic instability with the growth and shortening rates shown below. To account for the assumption that the poles search within a certain zone the width of which depends on the pole-to-pole distance, we introduced a spherical region with radius equal to

2 μm around each centrosome such that MTs from one pole invading this region around the other pole immediately catastrophe. This way, the poles search within certain cones in space such that MTs from opposite poles overlap little in space when the pole-to-pole distance is small, but mix more as the poles separate (Figure 5A). Starting with a given initial separation, the centrosomes in the simulations moved apart with a time-dependent velocity. From the data of Experiments 1-3 (Figures S3A, 4C-D), we extracted the pole-to-pole distances as functions of time and implemented these functions in the simulations. There are no spontaneous catastrophe and rescue events: rescues prolong MT growth in 'wrong' directions, while frequent catastrophes make it hard to capture properly KTs that are too far from poles (Wollman *et al.*, 2005). Instead, the MTs undergo catastrophe upon collisions with the nuclear space boundary. Unlike in (Paul *et al.*, 2009), we did not make the MTs catastrophe upon a collision with the chromosome arm, because this effect is not very important in the geometry considered here. Instead, the assumption was that MTs "slide off" the chromosome arms and continue to grow in a tangential direction.

In the simulations, syntelic MTs dissociate with the constant rate shown below, mero- and amphitelic connections are stable, and monotelic connections do not disassemble but can convert to syntelic or amphitelic ones. Importantly, we do not have fixed rates of making pole-KT connections. Instead, the connections are formed depending on the poles' and centrosomes' positions and MT numbers and growth/shortening rates. We found that the following assumptions had to be made to achieve good fit to the data shown in Figures 4C-E:

- Each KT has 2 binding sites for MTs. The first MT interacting with a KT has a binding probability 1, whereas for the second MT the binding rate is reduced to 0.5 (to account for the significant probability of other MTs nucleated or transported on the first attached MT

and saturating the second binding site). Having only two attachment sites is, of course, an over-simplification, because each KT binds 20-25 MTs (McEwen *et al.*, 1997), so we effectively think of MT bundles rather than individual MTs. Simulations with realistic numbers of the binding sites become too involved.

- Probability to establish the first, monotelic attachment increases linearly from zero to unity over a few minutes. This assumption can account for the gradual increase in the number of MTs involved in the search and increase in MT dynamicity for cells recovering from the drug treatments. Without this assumption, the fits are still good qualitatively, but quantitatively speaking, the assembly becomes too fast.
- We assume that monotelically attached chromosomes rotate, so that the non-captured KT faces away from the capturing pole (Rieder and Alexander, 1990; Nicklas, 1997). Because the MTs do not penetrate chromosome arms, this effect makes syntelic attachments less frequent than monotelic ones. This also reduces the number of merotelic attachments as the distance between the poles increases, so that the pole without a connection to the chromosome 'sees' the captured KT from such angle that the merotelic capture of this KT is less likely.
- Monotelically attached chromosomes move away from the poles to which they are connected, towards the spindle equator (Kapoor *et al.*, 2006; Cai *et al.*, 2009). This bias increases with growing pole-to-pole distance and effectively decreases the probability to establish a syntelic attachment but increases the probability to establish an amphitelic attachment with growing pole-to-pole distance.

- Effectively, the rotation and movement of the chromosomes create the following effects:
 - 1) the probability to establish a syntelic attachment decreases with the pole-to-pole distance, r , as $p(r) = (1 - r/r_{max})$; 2) the probability to establish a merotelic attachment decreases with the pole-to-pole distance, as $p(r) = (1 - r/r_{max})^2$; 3) the probability to establish an amphitelic attachment increases with the pole-to-pole distance, r , as $p(r) = (r/r_{max})$. Here r_{max} is the model parameter, maximal pole-to-pole separation (12-15 μm in the simulations; results are not sensitive to the exact value).

Parameters used in the simulations.

Number of chromosomes = 12; Number of MTs from each pole = 100;

KT length = 0.5 μm ; KT radius = 0.44 μm ;

Chromosome radius = 0.5 μm ; Chromosome length = 2 μm ;

MT growth rate = 0.18 $\mu\text{m/s}$; MT shortening rate = 1 $\mu\text{m/s}$;

Rate of dissociation of a syntelic MT = 0.5/min.

Stochastic Monte Carlo simulations using the algorithm and parameters described here were performed as described in (Paul *et al.*, 2009). The results are reported in Figures 5B-C and Figure S3B.

We also tested a number of modifications of the model:

- 1) In order to test a possible effect of plastic KTs (Loncarek *et al.*, 2007), we introduced varying random angles between the sister KTs and simulated spindle assembly with centrosomes starting at a distance of 0 μm . We found that the results did not fit the experimental data. Specifically, there was a dramatic decrease of amphitelic attachments from ~80% to less than 40%

and a respective increase in the number of mis-attachments (syn-, mono- and merotelic attachments). The reasons for that were “easy access” of MTs from both poles to unattached KTs, as well as more difficult access from the unconnected pole to the unattached KT of monotelic chromosomes. Note, that in our simulations, the angles between sister KTs varied but were static; it is entirely possible that a dynamic dependence of these angles on forces and/or attachments of MTs could remediate the errors of assembly. Moreover, in these simulations the angles between sister KTs were set at less than 180° before the establishment of any KT-MT interaction, but it is likely that this would not occur *in vivo* and that smaller angles would only be a consequence of prior establishment of syntelic attachment. However, our simulation results suggest that even in this case sister pairs that have previously established syntelic attachments would be unlikely to establish other types of attachments (mero- or amphitelic).

2) To test a possible effect of long K-fibers that could form during extensive pre-search (Khodjakov *et al.*, 2003), we repeated the simulations of Experiment 1 with an effective target size (representing increased target length as a sum of KT and K-fiber lengths) equal to $2\ \mu\text{m}$. The results are shown in Figure S3C; comparison with Figure S3B illustrates that the increase in the effective target size has very little effect. This is in agreement with the results reported in (Paul *et al.*, 2009) according to which the effective target size does not influence the accuracy of spindle assembly significantly. The K-fiber length is important for the speed of assembly on the scale of minutes, but on the scale of tens of minutes, characteristic for Experiment 1, this effect is not prominent.

3) In the simulations, the chromosome positions were not correlated with the centrosome positions, or with each other. We tried to introduce small unevenness in distributions of the chromosomes, and varied slightly restricted volumes within the oblate spheroid to which positions

of the chromosomes were limited and found that these changes did not affect the predicted time series for the spindle assembly. Greater inhomogeneity and/or restriction of the chromosomes to more confined spaces did perturb the results significantly, but there are no clear indications from our experimental data that such effects take place.

4) We simulated the scenario in which the tendency for monotelic chromosomes to move away from the capturing pole was delayed by a few minutes. Within the delay period, a few amphitelic chromosomes appear, so the monotelic chromosomes can move along respective k-fibers. Such delay did not change the results significantly.

5) We allowed MTs to search the whole space. The results (Figure S5A-B) compare poorly to the experimental data. However, when we at the same time allowed amphitelic and merotelic attachments to disassemble as a function of pole-to-pole distance – faster at small distances and slower at greater distances, the model predicted time series that better reproduce, despite residual discrepancies (see main text for details), the experimental data (Figure S5C-D). The rationale for such assumption is the possible effect of tension on the sister KTs exerted by attached MTs. Such tension depends on the angle between KTs connecting respective chromosomes to opposite poles, and therefore on the pole-to-pole distance. Specifically, we scaled the disassembly with probability of MT detachment equal to $P = 0.5 \times (1 - r/r_d)$ where r is the pole-to-pole distance, and $r_d = 3.5\mu\text{m}$ is the maximal distance at which this effect takes place.

Supplemental Figures

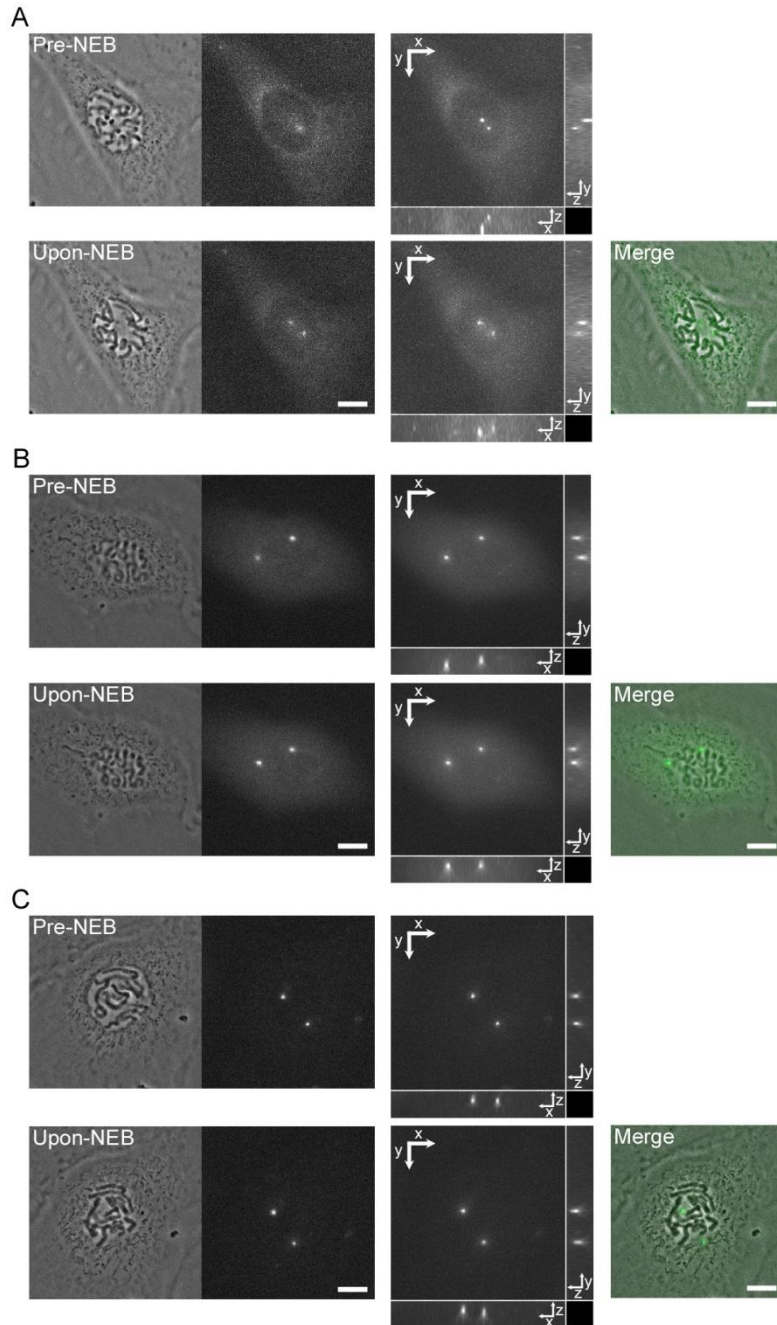


Figure S1. Examples of cells with incomplete centrosome separation at NEB. Examples of the three centrosome configurations [Top-bottom (A); side-side (B); top-side (C)] depicted in Figures 1A-Bii-iv in PtK1 cells expressing GFP- γ -tubulin. For each example, images of the cell prior to NEB (Pre-NEB) are shown in the top row and images of the cell upon NEB (Upon-NEB) are shown in the bottom row. Images of chromosomes and centrosomes at a single focal plane are shown in the first and second column, respectively. Maximum intensity projections in XY accompanied by YZ and XZ views are shown in the third column. The far-right column displays the overlay of phase contrast and fluorescence images at a single focal plane upon NEB. Scale bars, 5 μm .

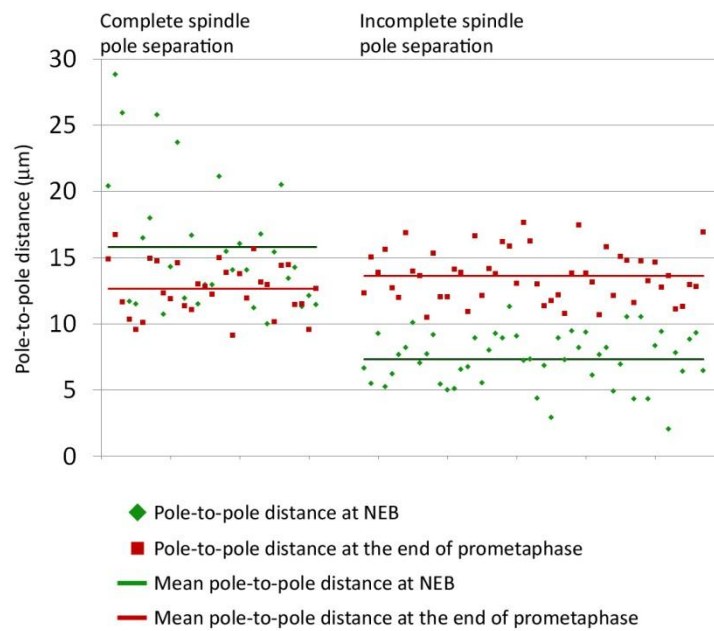


Figure S2. Pole-to-pole distance in *PtK1* cells with complete vs. incomplete centrosome separation at NEB. Pole-to-pole measurements were obtained both upon NEB and at the end of prometaphase for all *PtK1* cells imaged during the experiments summarized in figures 1 and 2.

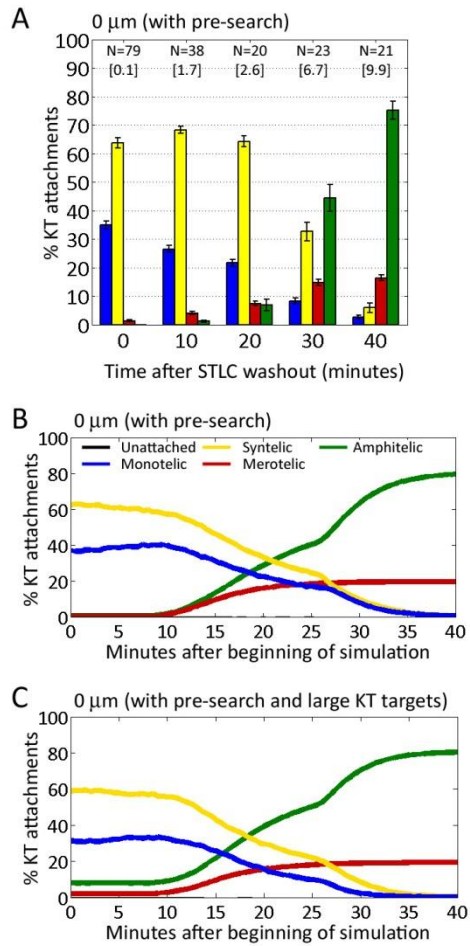


Figure S3. The size of the KT target does not affect the numbers and types of KT attachments in cells recovering from a 2-hour STLC treatment. (A) Frequencies of different types of KT attachments in cells washed-out of STLC after a 2-hr treatment. In these cells, the spindle poles gradually separated after persisting in very close proximity for 2 hrs and establishing KT attachment (spindle poles moving apart from 0 μm , with a 2-hr period of pre-search). N represents the number of cells analyzed. The numbers in square brackets represent the average pole-to-pole distance (in μm) at each time-point. (B) Computer simulation of spindle bipolarization with spindle poles starting at a distance of 0 μm after a 2-hr pre-search period (as in the experiment in A). (C) Computer simulation of spindle bipolarization under conditions identical to those used in B, except for the KT target size, which was set to 2 μm , as opposed to 0.5 μm in B.

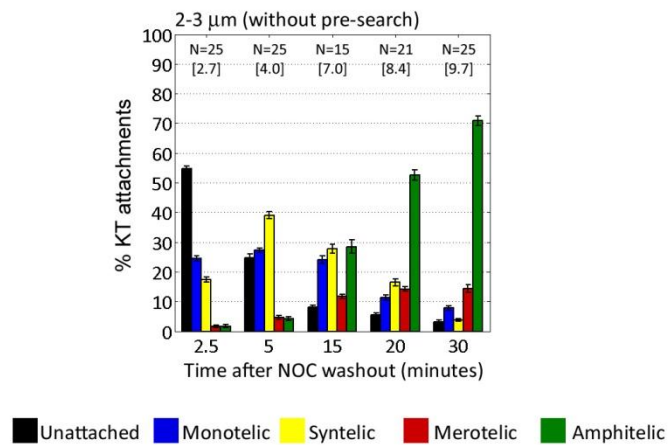


Figure S4. *Frequencies of different types of KT attachments in PtK1 cells with an initial pole-to-pole distance of 2-3 μm . Cells were first treated with STLC for 2 hrs, then washed out and re-incubated in STLC-free media for 15 min (to allow spindle poles to move apart to an average distance of 2-3 μm), then incubated in NOC for 30 min, and finally washed out of the NOC and fixed at subsequent time-points. N represents the number of cells analyzed. The numbers in square brackets represent the average pole-to-pole distance (in μm) at each time-point.*

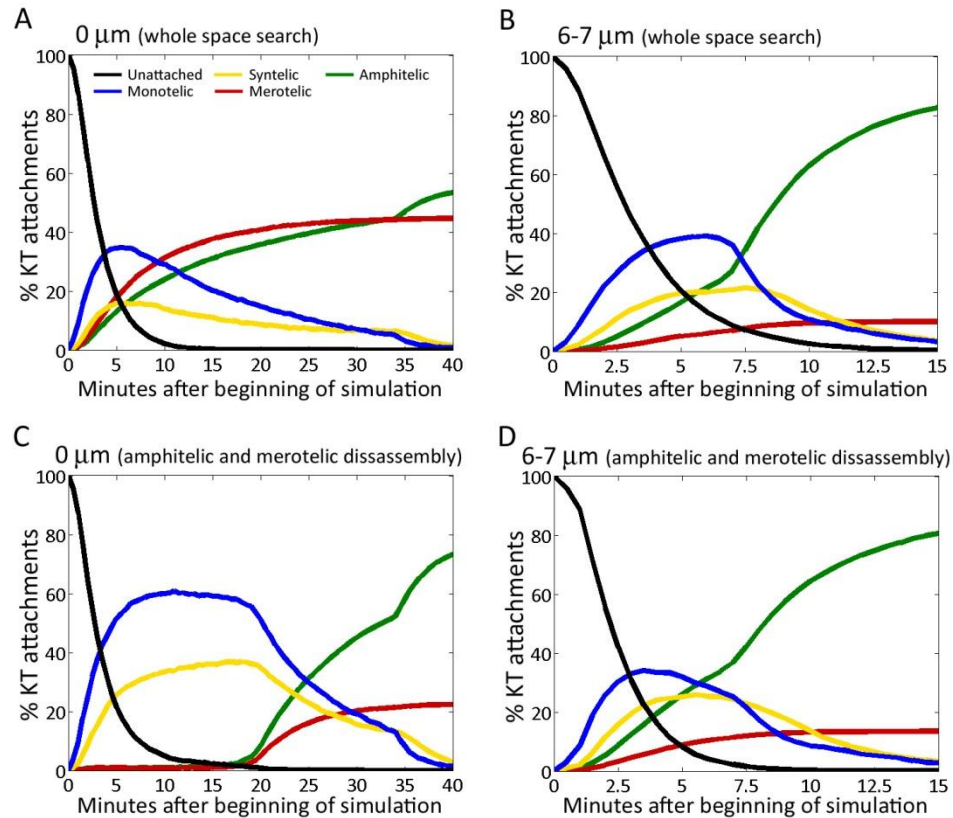


Figure S5. Computer simulations of spindle assembly without shielding effect can reproduce experimental results only if merotelic and amphitelic KT attachments disassemble at very high rates at small pole-to-pole distances. (A-B) Time-course simulations of spindle assembly in the absence of shielding effect between the two centrosomes (whole-space search). (A) Simulation starting with a spindle pole distance of $0\ \mu\text{m}$ without pre-search (as in figure 4C). (B) Simulation starting with a spindle pole distance of $6\ \mu\text{m}$ without pre-search (as in figure 4D). Whereas the simulation results at the initial distance of $6\ \mu\text{m}$ fit the experimental results, the simulation results for an initial distance of $0\ \mu\text{m}$ are very different from the experimental results. (C-D) Time-course simulations of spindle assembly with whole-space search and rapid disassembly of merotelic and amphitelic attachments at small pole-to-pole distances. (C) Simulation starting with a spindle pole distance of $0\ \mu\text{m}$ without pre-search (as in figure 4C). (D) Simulation starting with a spindle pole distance of $6\ \mu\text{m}$ without pre-search (as in figure 4D). At the initial pole-to-pole distance of $6\ \mu\text{m}$ the simulation results fit well the experimental results, but that is not the case for an initial pole-to-pole distance of $0\ \mu\text{m}$.

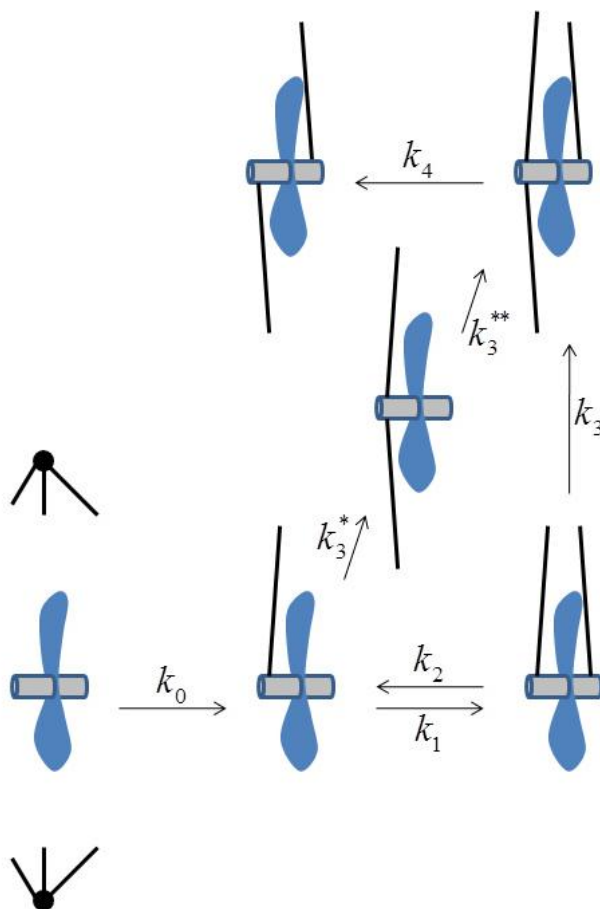


Figure S6. Possible pathways of establishment of KT attachment during simulation of approximate kinetics of spindle assembly. All the KTs are unattached (bottom left) at the beginning of the simulation. Merotelic and correct amphitelic attachments can be achieved through different pathways.

Supplemental References

Cai, S., O'Connell, C.B., Khodjakov, A., and Walczak, C.E. (2009). Chromosome congression in the absence of kinetochore fibres. *Nat Cell Biol* *11*, 832-838.

Cimini, D. (2007). Detection and correction of merotelic kinetochore orientation by Aurora B and its partners. *Cell Cycle* *6*, 1558-1564.

Kapoor, T.M., Lampson, M.A., Hergert, P., Cameron, L., Cimini, D., Salmon, E.D., McEwen, B.F., and Khodjakov, A. (2006). Chromosomes can congress to the metaphase plate before biorientation. *Science* *311*, 388-391.

Khodjakov, A., Copenagle, L., Gordon, M.B., Compton, D.A., and Kapoor, T.M. (2003). Minus-end capture of preformed kinetochore fibers contributes to spindle morphogenesis. *J Cell Biol* *160*, 671-683.

Loncarek, J., Kisurina-Evgenieva, O., Vinogradova, T., Hergert, P., La Terra, S., Kapoor, T.M., and Khodjakov, A. (2007). The centromere geometry essential for keeping mitosis error free is controlled by spindle forces. *Nature* *450*, 745-749.

McEwen, B.F., Heagle, A.B., Cassels, G.O., Buttle, K.F., and Rieder, C.L. (1997). Kinetochore fiber maturation in PtK1 cells and its implications for the mechanisms of chromosome congression and anaphase onset. *J Cell Biol* *137*, 1567-1580.

Mogilner, A., and Craig, E. (2010). Towards a quantitative understanding of mitotic spindle assembly and mechanics. *J Cell Sci* *123*, 3435-3445.

Nicklas, R.B. (1997). How cells get the right chromosomes. *Science* *275*, 632-637.

Paul, R., Wollman, R., Silkworth, W.T., Nardi, I.K., Cimini, D., and Mogilner, A. (2009). Computer simulations predict that chromosome movements and rotations accelerate mitotic spindle assembly without compromising accuracy. *Proc Natl Acad Sci U S A* *106*, 15708-15713.

Rieder, C.L., and Alexander, S.P. (1990). Kinetochores are transported poleward along a single astral microtubule during chromosome attachment to the spindle in newt lung cells. *J Cell Biol* *110*, 81-95.

Wollman, R., Cytrynbaum, E.N., Jones, J.T., Meyer, T., Scholey, J.M., and Mogilner, A. (2005). Efficient chromosome capture requires a bias in the 'search-and-capture' process during mitotic-spindle assembly. *Curr Biol* *15*, 828-832.